1 **Regulation of γ-aminobutyrate (GABA) utilization in**

2 ***Corynebacterium glutamicum* by the PucR-type transcriptional**

3 **regulator GabR and by alternative nitrogen and carbon sources**

4

5 **Lingfeng Zhu[#], Christina Mack, Astrid Wirtz, Angela Kranz, Tino Polen, Meike**

6 **Baumgart[*], and Michael Bott[*]**

7

8 IBG-1: Biotechnology, Institute of Bio- and Geosciences, Forschungszentrum Jülich, Jülich,

9 Germany

10

11 **Running title:** Regulation of corynebacterial GABA utilization

12

13 ***Correspondence:** Michael Bott (m.bott@fz-juelich.de) or Meike Baumgart

14 (m.baumgart@fz-juelich.de)

15

16 [#]Current address: Center for Synthetic Biochemistry, Institute of Synthetic Biology,

17 Shenzhen Institutes of Advanced Technologies, Chinese Academy of Sciences, Shenzhen,

18 China

19

20 ORCID Ling-Feng Zhu   0000-0002-9145-5419

21 ORCID Christina Mack   0000-0002-3495-3796

22 ORCID Astrid Wirtz   0000-0003-2159-3717

23 ORCID Angela Kranz   0000-0002-8000-0400

24 ORCID Tino Polen   0000-0002-0065-3007

25 ORCID Meike Baumgart   0000-0002-9874-1151

26   ORCID Michael Bott   0000-0002-4701-8254

27

28   For the microarray data, the following secure token has been created to allow review of

29   GEO record GSE138829 while it remains in private status: ahupaoiipdeprol

30   https://www.ncbi.nlm.nih.gov/geo/query/acc.cgi?acc=GSE138829

31   For the RNAseq data, the following secure token has been created to allow review of

32   GEO record GSE156688 while it remains in private status: gfirgmimfhwzfkh

33   https://www.ncbi.nlm.nih.gov/geo/query/acc.cgi?acc=GSE156688

34

ABSTRACT

γ-Aminobutyric acid (GABA) is a non-proteinogenic amino acid mainly formed by decarboxylation of L-glutamate and is widespread in nature from microorganisms to plants and animals. In this study, we analyzed the regulation of GABA utilization by the Gram-positive soil bacterium *Corynebacterium glutamicum*, which serves as model organism of the phylum *Actinobacteria.* We show that GABA usage is subject to both specific and global regulatory mechanisms. Transcriptomics revealed that the *gabTDP* genes encoding GABA transaminase, succinate semialdehyde dehydrogenase, and GABA permease, respectively, were highly induced in GABA-grown cells compared to glucose-grown cells. Expression of the *gabTDP* genes was dependent on GABA and the PucR-type transcriptional regulator GabR, which is encoded divergently to *gabT*. A Δ*gabR* mutant failed to grow with GABA, but not with glucose. Growth of the mutant on GABA was restored by plasmid-based expression of *gabR* or of *gabTDP*, indicating that no further genes are specifically required for GABA utilization. Purified GabR (calculated mass 55.75 kDa) formed an octamer with an apparent mass of 420 kDa and bound to two inverted repeats in the *gabR-gabT* intergenic region. Glucose, gluconate, and *myo*-inositol caused reduced expression of *gabTDP*, presumably via the cAMP-dependent global regulator GlxR, for which a binding site is present downstream of the *gabT* transcriptional start site. *C. glutamicum* was able to grow with GABA as sole carbon and nitrogen source. Ammonium and, to a lesser extent, urea inhibited growth on GABA, whereas L-glutamine stimulated it. Possible mechanisms for these effects are discussed.

Keywords: *Corynebacterium glutamicum*, *Actinobacteria*, γ-aminobutyrate, PucR-type regulator GabR, cAMP-dependent regulator GlxR, nitrogen metabolism, carbon metabolism

INTRODUCTION

γ-Aminobutyric acid (GABA) is a non-proteinogenic amino acid, which is widespread in nature from microorganisms to plants and animals. GABA is formed by many gram-negative and gram-positive bacteria as part of the acid stress response (Cotter and Hill, 2003; Foster, 2004; Krulwich et al., 2011; De Biase and Pennacchietti, 2012). The irreversible decarboxylation of L-glutamate by glutamate decarboxylase results in the formation of GABA and carbon dioxide and consumes a proton within the cytoplasm, thereby acting against acid stress. An antiporter takes up L-glutamate and exports GABA. This acid stress response can also start from L-glutamine, which is first converted to L-glutamate and ammonia by a glutaminase (Pennacchietti et al., 2018). The human gut microbiome contains several GABA-producing or GABA-consuming species, and there might be a connection between GABA production in the gut and depressive disorders (Strandwitz et al., 2019). In plants, GABA plays a role in stress responses and at the interface of carbon and nitrogen metabolism (Michaeli and Fromm, 2015). In the brain of mammals, GABA is an important neurotransmitter (Abdou et al., 2006; Ben-Ari et al., 2007). GABA has also gained much attention as a building block for the synthesis of 2-pyrrolidone and the biodegradable polyamide nylon 4 (Kawasaki et al., 2005). Therefore, microbial synthesis of GABA has frequently been studied (Krulwich et al., 2011; Dhakal et al., 2012; Jorge et al., 2016; Xu et al., 2017).

Due to its widespread occurrence in nature, GABA can be used by many bacteria as carbon and nitrogen source. After uptake by specific transporters (usually named GabP), a transaminase (GabT) converts GABA and 2-oxoglutarate in a pyridoxal 5-phosphate (PLP)-dependent reaction to succinate semialdehyde and glutamate. Succinate semialdehyde is then oxidized by an $NAD(P)^+$-dependent succinate semialdehyde dehydrogenase (GabD) to succinate, an intermediate of the central metabolism (Scott and Jakoby, 1958; Dover and Halpern, 1972; Feehily and Karatzas, 2013). Despite the fact that many bacteria possess the characteristic genes involved in GABA metabolism, their regulation has so far only been

4

85   studied in a few species such as *Bacillus subtilis*, *Bacillus thuringiensis*, or *Escherichia coli*.

86   The best-studied regulator is probably GabR of *B. subtilis* (designated here GabR$_{Bs}$), which

87   belongs to the MocR/GabR subfamily of the GntR family of transcriptional regulators

88   (Edayathumangalam et al., 2013; Wu et al., 2017). GabR$_{Bs}$ consists of an N-terminal helix-turn-

89   helix (HTH) domain and a C-terminal aminotransferase domain and activates its target genes

90   *gabTD* in the presence of GABA and PLP (Belitsky, 2004). Surprisingly, in the close relative

91   *B. thuringiensis*, the regulation of GABA metabolism is different. Here, the regulator GabR$_{Bt}$

92   belongs to the family of bacterial enhancer binding proteins that function as activators of σ^{54}-

93   dependent promoters. GabR$_{Bt}$ is composed of a Per-ARNT-Sim (PAS) domain, a σ^{54} interaction

94   domain, and a C-terminal HTH domain and activates its target gene *gabT* in the presence of

95   GABA and succinate semialdehyde (Zhu et al., 2010; Peng et al., 2014). In *E. coli*, the genes

96   *gabTDP* are presumably organized in an operon *gabTDPC* together with *gabC*, and activated

97   under nitrogen limitation by the Nac regulator (Schneider et al., 2002). The product of *gabC* is

98   a transcriptional regulator belonging to the FadR subfamily of the GntR family of

99   transcriptional regulators and seems to repress this operon. However, the exact physiological

100   function of GabC$_{Ec}$ is unclear up to now (Schneider et al., 2002). GABA is also an intermediate

101   of putrescine degradation to succinate in *E. coli*, which involves PuuE as isoenzyme of GabT

102   and PuuC as isoenzyme of GabD (Kurihara et al., 2010; Schneider and Reitzer, 2012). In

103   summary, the regulation of genes involved in GABA metabolism appears to be rather diverse

104   in bacteria.

105   *Corynebacterium glutamicum* is a gram-positive soil bacterium widely used for the industrial

106   production of amino acids, in particular the flavor enhancer L-glutamate and the feed additive

107   L-lysine (Eggeling and Bott, 2005). The wild type is unable to synthesize GABA, but

108   recombinant strains for GABA production were constructed (Shi and Li, 2011; Takahashi et

109   al., 2012; Shi et al., 2013; Jorge et al., 2016). In the course of these studies, it became clear that

110   *C. glutamicum* is able to degrade GABA and a number of proteins involved in this process were

studied (Fig. 1). GabP (Cg0568) is a secondary Na^+-dependent transporter for GABA uptake with a K_m value of 34.2 ± 1.1 μM and a V_{max} of 67.3 ± 1.0 nmol min^{-1} (mg cell dry weight)$^{-1}$ at pH 7.5 and essential for GABA utilization (Zhao et al., 2012). GabT (Cg0566) is a GABA transaminase and the purified enzyme has a specific activity of 1.34 U/mg protein and K_m values of 10.65 mM for GABA and 9.21 mM for 2-oxoglutarate (Shi et al., 2017). GabT was shown to be a tetramer and the crystal structure in complex with PLP-GABA allowed the identification of the key residues that contribute to the formation of the active site (Hong and Kim, 2019). Since a *gabT* deletion strain was still able to degrade GABA, the presence of another transaminase catalyzing this reaction was suggested (Ni et al., 2015). The protein encoded by *bioA* (cg2885) was recently reported to possess GABA transaminase activity, but the specific activity of the purified BioA enzyme was only 2% of the GabT activity (Shi et al., 2017). With respect to succinate semialdehyde dehydrogenase, three genes were annotated to encode this enzyme, namely *gabD* (cg0566), cg0067, and cg3004 (Fig. 1) (Kalinowski et al., 2003). None of the corresponding proteins has been biochemically characterized to our knowledge.

In this study, our aim was to investigate the regulation of GABA utilization in *C. glutamicum*. We show that the *gabTDP* operon is regulated by a specific transcriptional regulator, GabR, which does not belong to the regulator families described above for GabR proteins of other bacteria, but to the PucR family, further confirming the heterogeneity in transcriptional regulation of the genes involved in GABA transport and metabolism. GabR presumably requires GABA for transcriptional activation, but not for DNA-binding. The *gabTDP* operon is probably also regulated by the cAMP-dependent global regulator GlxR, which is proposed to repress expression when alternative carbon sources are present. Besides alternative carbon sources, also alternative nitrogen sources have a profound influence on GABA utilization, with ammonium and urea acting as inhibitors and glutamine serving as stimulator.

MATERIALS AND METHODS

Bacterial strains, plasmids and growth conditions

The bacterial strains and plasmids used in this study are listed in Table 1. The *C. glutamicum*
ATCC 13032 type strain served as wild type (WT). *C. glutamicum* was routinely cultivated at
30 °C. For precultivation of *C. glutamicum*, brain heart infusion (BHI) medium (Becton
Dickinson GmbH, Heidelberg, Germany) with 90 g L^{-1} sorbitol was used. The cells of these
precultures were harvested by centrifugation (5,000*g*, 4 °C, 10 min), and washed twice with
phosphate buffer (100 mM KH$_2$PO$_4$/Na$_2$HPO$_4$ pH 7.0). Growth experiments were routinely
performed in a BioLector microcultivation system (m2p-labs, Baesweiler, Germany) using 48-
well FlowerPlates (m2p-labs) containing 750 μL CGXII minimal medium (Keilhauer et al.,
1993) containing 30 mg L^{-1} protocatechuic acid as iron chelator. In the BioLector, growth of
the cells is measured as scattered light at 620 nm (Kensy et al., 2009a; Kensy et al., 2009b).
Please note that the absolute backscatter values of the graphs in this manuscript differ because
of the use of different instruments. Due to this, reference cultures were always included to allow
comparison between different experiments. For determination of GABA and glucose
consumption, cells were cultured in 500-mL baffled shake flasks with 50 mL medium that were
incubated at 30 °C and 130 rpm (see Fig. 8). *E. coli* was grown at 37 °C in lysogeny broth
(Bertani, 1951). When required for plasmid maintenance, media were supplemented with
kanamycin (50 μg mL^{-1} for *E. coli*, 25 μg mL^{-1} for *C. glutamicum*) or chloramphenicol (20 μg
mL^{-1}).

Recombinant DNA work and construction of deletion mutants

Routine methods such as PCR, DNA restriction and ligation were performed using standard
protocols (Sambrook et al., 1989; van der Rest et al., 1999). All oligonucleotides used in this
study are listed in Table S1 and were synthesized by Eurofins Genomics (Ebersberg, Germany).
The enzymes for recombinant DNA work were obtained from New England Biolabs (Frankfurt,

162 Germany) and Thermo Fisher Scientific (Vilnius, Lithuania). The correctness of the insert

163 sequences of all recombinant plasmids was verified by DNA sequencing (Eurofins Genomics,

164 Ebersberg, Germany).

165   The *C. glutamicum* Δ*gabR* strain was constructed by allelic exchange using the plasmid

166 pK19*mobsacB* (Schäfer et al., 1994) as described before (Niebisch and Bott, 2001). For

167 construction of pK19*mobsacB*-Δ*gabR,* the oligonucleotide pairs cg0565frontF/R and

168 cg0565backF/R were used to amplify DNA regions of approximately 500 bp upstream and

169 downstream of *gabR* using *C. glutamicum* WT genomic DNA as template. The resulting PCR

170 products were fused by Gibson assembly (Gibson et al., 2009) with pK19*mobsacB* which had

171 been digested with *Bam*HI and *Pst*I. After successful construction, pK19*mobsacB*-Δ*gabR* was

172 used to transform competent *C. glutamicum* WT. The transformed cells were first selected for

173 kanamycin resistance and subsequently for tolerance toward sucrose. Successful deletion of

174 *gabR* was confirmed by colony PCR with the oligonucleotides cg0565checkF and

175 cg0565checkR, which anneal outside of the deleted regions. Out of six analyzed clones, three

176 showed the desired *gabR* deletion, while three clones represented the WT situation.

177   For construction of plasmid pAN6-*gabR*, the *gabR* coding region was amplified by PCR

178 using the oligonucleotides 0565F and 0565R and chromosomal DNA of *C. glutamicum* WT as

179 template. After digestion with *Nde*I and *Nhe*I, the PCR product was cloned into the expression

180 plasmid pAN6 cut with the same restriction enzymes using the Rapid DNA Ligation Kit (Roche

181 Diagnostics, Mannheim, Germany). The plasmid pET-TEV-*gabR* was constructed similar to

182 pAN6-*gabR*. The *gabR* gene was amplified with the oligonucleotides 0565F and petfhis0565R,

183 the PCR product was digested with *Nde*I and *Hin*dIII and ligated with pET-TEV cut with the

184 same restriction enzymes. For construction of plasmid pAN6-*gabTDP*, the genes *gabTDP*, were

185 amplified by PCR using the oligonucleotide pair gabtdpF/gabtdpR and chromosomal DNA of

186 *C. glutamicum* WT as template. The resulting PCR product was fused with pAN6 cut with *Nde*I

187 and *Nhe*I by Gibson assembly.

188   For construction of plasmid pJC1-P$_{gabT}$-eYFP, a 500-bp fragment covering the *gabTDP*

189   promoter region immediately upstream of the *gabT* start codon was amplified using the

190   oligonucleotide pair PgabTF/PgabTR with genomic DNA of *C. glutamicum* WT as template.

191   The eYFP-encoding gene was amplified with the oligonucleotide pair eYFPF/eYFP-termR and

192   plasmid DNA of pJC1-P$_{tac}$-*eyfp* as template. The two PCR fragments were fused by Gibson

193   assembly with pJC1-venus-term, which had been digested with *Bam*HI and *Spe*I.

194

DNA microarray analysis

196   Comparative transcriptome analysis using DNA microarrays was performed as described

197   previously (Vogt et al., 2014) , except that $(NH_4)_2SO_4$ was omitted from the medium to exclude

198   ammonium and 20 mM K_2SO_4 was added to avoid a possible sulfate limitation. The medium

199   still contains 83 mM urea as nitrogen source. *C. glutamicum* WT was cultivated in this modified

200   medium with either 62.5 mM GABA or with 41.7 mM glucose as carbon source, corresponding

201   to 250 mM C. When an optical density at 600 nm (OD$_{600}$) of 5 was reached (measured with an

202   Ultrospec 2100pro spectrophotometer (Biochrom, Berlin, Germany)), the cells were harvested

203   by centrifugation (4000*g*, 10 min, 4 °C). The cell pellet was subsequently frozen in liquid

204   nitrogen and stored at −80 °C. Total RNA isolation of *C. glutamicum* cells was performed using

205   the RNeasy Mini kit (Qiagen, Hilden, Germany), and the RNA was kept at −80 °C until further

206   use. Fluorescently labeled cDNA copies of total RNA of *C. glutamicum* were prepared using

207   SuperScript III reverse transcriptase (Life Technologies, Darmstadt, Germany). To remove

208   unincorporated fluorophores, the probes were purified using Amicon Centrifugal Filters (Merck

209   Millipore, Darmstadt, Germany). The cDNA probes labeled with Cy3 and Cy5 were hybridized

210   using Agilent's Gene Expression Hybridization Kit (Waldbronn, Germany), hybridization oven

211   and hybridization chamber. After 16 h of hybridization at 65 °C, the microarrays were washed

212   using Agilent's Wash Buffer Kit according to the manufacturer's instructions. Signal

213   acquisition was performed with a GenePix 4000B laser scanner and GenePix Pro 7.0 software

214 (Molecular Devices, Sunnyvale, CA, USA). For background correction of spot intensities, ratio

215 calculation and ratio normalization, data were processed using the BioConductor R-packages

216 limma and marray (http://www.bioconductor.org). The full microarray data sets of this study

217 have been deposited in the NCBI Gene Expression Omnibus and can be found under the GEO

218 accession number GSE138829.

219

220 Determination of the transcriptional start sites (TSSs)

221 The TSS of *gabT* was initially determined using the 5′/3′ RACE Kit (Roche Diagnostics,

222 Mannheim, Germany). In brief, RNA was extracted from *C. glutamicum* WT cells cultivated

223 with GABA as sole carbon and nitrogen source using an RNeasy Mini Kit (Qiagen). Then.

224 transcription of specific mRNA sequences into first-strand cDNA was performed using the

225 extracted RNA and oligonucleotide GABTTS1R (Table S1). A homopolymeric A-tail was

226 added to the 3´-end of the first-strand cDNA using recombinant terminal transferase and dATP.

227 Finally, the amplification of dA-tailed cDNA was performed using first and second round PCR

228 using the primers GABTTS2R and GABTTS3R, respectively (Table S1). The PCR products

229 were sequenced to determine the TSS. The TSS determination was performed independently

230 for three biological replicates.

231　In an alternative approach, the TSSs present within the *gabR-gabTDP* region were

232 analyzed by RNAseq using RNA of WT cells cultivated with GABA as sole carbon and energy

233 source. Three independent cultures (5 ml BHI) were inoculated with a single colony from a

234 fresh agar plate and cultivated at 30 °C and 170 rpm during the day. The cells were washed two

235 times with 0.9% (w/v) NaCl and used to inoculate the second precultures of 20 ml CGXII

236 medium with 2% (w/v) glucose in a 1:100 dilution. These cultures were cultivated at 30°C and

237 130 rpm overnight. For the main cultures, 50 ml CGXII medium without ammonium and urea

238 but with 62.5 mM GABA as carbon and nitrogen source were inoculated with the precultures

239 to an OD_{600} of 1. The main cultures were incubated at 30 °C and 130 rpm and harvested after 6

10

240   h at an OD_{600} of 2.5-2.7. RNA isolation was performed with the RNeasy Mini Kit (Qiagen,

241   Hilden, Germany). For the sequencing, RNA of all three cultures was mixed in equal amounts.

242   Further RNA processing and sequencing was performed by Vertis Biotechnologie AG

243   (Freising-Weihenstephan, Germany). Processing and mapping of the 10,117,524 single-end

244   sequenced reads was performed with the CLC Genomics Workbench (Qiagen Aarhus A/S).

245   Reads were trimmed by removing adapter sequences using the Trim Sequences tool and filtered

246   for Phred quality scores <30 (Ewing and Green, 1998). Trimmed reads (10,052,707) were

247   mapped to the *C. glutamicum* reference sequence (BX927147). Automatic detection of TSSs

248   was done with ReadXplorer (Hilker et al., 2014) using the following parameters: (i) Only single

249   perfect mappings without errors were considered. (ii) Minimum percentage of coverage

250   increase was set to 100% and minimum number of reads starts to 20. Every possible TSS for

251   cg0565-cg0568 was manually checked including TSS with less than 20 reads.

252

253   **Protein production and purification**

254   For GabR production and purification, *E. coli* BL21(DE3) harboring pET-TEV-*gabR* was first

255   cultivated in 5 mL LB medium with 50 µg mL^{-1} kanamycin in 20 mL glass tubes at 37 °C with

256   shaking overnight. Subsequently, 2 mL preculture was used to inoculate 200 mL LB medium

257   with kanamycin in a 500 mL shake flask, which was cultivated at 37 °C and 120 rpm. When

258   the culture reached an OD_{600} of 0.6, 0.2 mM isopropyl β-D-1-thiogalactopyranoside (IPTG) was

259   added to induce *gabR* expression. After induction, the cells were further cultivated at 16 °C for

260   8 h and harvested by centrifugation (4,000g, 10 min, 4 °C). The harvested cells were suspended

261   in binding buffer (20 mM Tris-HCl, 500 mM NaCl, 1 mM DTT, 10 mM imidazole, pH 7.8) and

262   disrupted by sonication for 20 minutes while cooling on ice with a UP 200 S ultrasonic device

263   (Hielscher, Germany) using a power amplitude of 55% and a pulse cycle of 0.3. The resulting

264   cell extract was centrifuged at 12,000g for 20 min to remove cell debris and the supernatant

265   was subjected to Ni^{2+} affinity chromatography using Ni-NTA Superflow (Qiagen, Hilden,

266 Germany). The column was equilibrated with binding buffer. After adding the cell-free extract,

267 the column was washed first with three column volumes of binding buffer and then with three

268 column volumes of wash buffer (20 mM Tris-HCl, 500 mM NaCl, 1 mM DTT, 80 mM

269 imidazole, pH 7.8). GabR protein with an N-terminal decahistidine tag was eluted with elution

270 buffer (20 mM Tris-HCl, 500 mM NaCl, 1 mM DTT, and 300 mM imidazole, pH 7.8).

271 Subsequently, the His-tag was cleaved off with tobacco etch virus (TEV) protease (Kapust and

272 Waugh, 1999) by incubation of 12 mg His-tagged GabR with 0.24 mg His-tagged TEV protease

273 overnight at 4 °C in TEV buffer (25 mM Tris-HCl, pH 8.0, 0.25 mM EDTA, 1 mM DTT).

274 Subsequently, GabR was further purified by gel filtration with a Superdex™ 200 increase

275 10/300 GL column (GE Healthcare, Freiburg, Germany) connected to an Äkta™ Pure25 system

276 (GE Healthcare) using 100 mM phosphate buffer pH 7.0 with 1 mM DTT and a flow rate of

277 0.75 mL min^{-1}. The elution volumes of the standard proteins were 9.41 mL for thyroglobulin

278 (669 kDa), 10.87 mL for apoferritin (443 kDa), 12.06 mL for amylase (200 kDa), 12.85 mL for

279 alcohol dehydrogenase (150 kDa), 14.27 ml for BSA (66 kDa), 16.26 mL for carbonic

280 anhydrase (29 kDa), and 17.34 mL for cytochrome c (12.4 kDa).

281 Overproduction and purification of the transaminase GabT were performed according to a

282 previous publication (Marienhagen et al., 2005). *E. coli* BL21(DE3) carrying plasmid pJM0462

283 was precultivated in 5 mL LB medium with 20 µg mL^{-1} chloramphenicol in 20 mL tubes at

284 37 °C and 120 rpm overnight. Subsequently, 2 mL preculture was used to inoculate 200 mL LB

285 medium with 20 µg mL^{-1} chloramphenicol in a 500 mL shake flask, which was cultivated at

286 37 °C and 120 rpm. Induction of target gene expression was induced by addition of 20 µL

287 anhydrotetracycline (2 mg (mL ethanol)$^{-1}$) when the cultures had reached an OD$_{600}$ of 0.4 to 0.6

288 and the cultures were further incubated for 8 h at 16 °C. Crude extracts were obtained by

289 sonication while cooling on ice. After removal of the cellular debris by centrifugation (15 min,

290 16,000g, 4 °C), protein purification was performed by affinity chromatography on ice using

291 Strep-TactinXT Sepharose (IBA, Göttingen, Germany). Buffer W (100 mM Tris-HCl pH 8.0,

292   150 mM NaCl, 1 mM EDTA) was used for equilibration and washing, and buffer BXT (buffer

293   W containing 50 mM biotin) was used for elution. The purified proteins were analyzed by SDS-

294   PAGE. Protein concentrations were determined using the BC Protein Assay Kit (Interchim

295   Uptima, Montlucon Cedex, France) with bovine serum albumin (BSA) as standard.

296

297   **Electrophoretic mobility shift assays (EMSAs)**

298   EMSAs were performed as described previously (Wennerhold and Bott, 2006). The DNA

299   fragments (100 ng, 30 – 500 bp) were incubated with purified GabR protein (0 – 2.6 µM

300   monomer) in binding buffer (10 mM Tris-HCl pH 7.5, 50 mM NaCl, 5% (v/v) glycerol, 0.005%

301   (v/v) Triton X-100) for about 20 min at room temperature. Electrophoresis was performed using

302   6% or 8% (w/v) native polyacrylamide gels in an ice bath with TB buffer (89 mM Tris-HCl pH

303   8.2, 89 mM boric acid) as running buffer. A pre-run without samples was carried out, so that

304   buffer differences between the gel and the running buffer were adjusted (180 V, 1.5 h). After

305   the pre-run, the samples were mixed with sample buffer (0.01% (w/v) xylene cyanol, 0.01%

306   (w/v) bromophenol blue, 20% (v/v) glycerol, in 1× TB buffer) and loaded onto the gel.

307   Electrophoresis was performed with the same conditions as the pre-run for 40 minutes and the

308   gels were subsequently stained with SYBR green (Sigma-Aldrich, Darmstadt, Germany).

309

310   **HPLC analysis of GABA and glucose**

311   For the determination of GABA and glucose in culture superntants, 1-mL culture aliquots were

312   taken at selected time points, centrifuged for 5 min at 13,000g, and the supernatant was stored

313   at -20 °C. Thawed samples were filtered (0.2 µm syringe filter, Whatman[TM], GE Healthcare,

314   Freiburg, Germany) prior to HPLC analysis. The GABA concentration was quantified as *ortho-*

315   phthalaldehyde derivative by reverse phase chromatography using an Agilent 1290 Infinity I

316   LC system (Agilent, Santa Clara, USA) equipped with a 5-micron 4.6 × 12.5 mm protective

317   column and a Zorbax Eclipse AAA 3.5 micron 4.6 × 75 mm separating column. A gradient of

318   sodium borate buffer (A: 10 mM Na_2HPO_4, 10 mM $Na_2B_4O_7$, pH 8.2) and methanol (B) was

319   used as eluent. Starting initially with 100% A, B was increased within 9.8 min from 0% to 57%.

320   At 10 min, B was set to 100% and hold for 2.5 min. Re-equilibration to 100% A was started

321   after 12.5 min and terminated after 14 min. The *ortho*-phthalaldehyde derivative was detected

322   by a fluorescence detector using an excitation wavelength of 340 nm and an emission

323   wavelength of 450 nm. The flow rate was 2 mL/min and the temperature was kept constant at

324   40°C.

325   Glucose was quantified essentially as described (Richhardt et al., 2012) using an Agilent

326   LC-1100 system (Agilent, Santa Clara, CA, USA) equipped with a Carbo-Ca Guard Cartridge

327   (Phenomenex, Aschaffenburg, Germany) and a Rezex^{TM} RCM-Monosaccharide 300 x 7.8 mm

328   column (Phenomenex, Aschaffenburg, Germany). Separation was performed at 80 °C with

329   water as eluent at a flow rate of 0.6 mL/min. Glucose was detected with a refraction index

330   detector (35 °C). Glucose was calibrated in a range of 0.1 to 8 g/L, with a retention time of 11.2

331   min.

332

333   **Assay for GABA transaminase activity**

334   The activity of GABA transaminase was measured as described (Marienhagen et al., 2005).

335   Briefly, the assay buffer contained 200 mM Tris-HCl pH 8, 0.25 mM pyridoxal 5'-phosphate,

336   20 mM GABA, and 20 mM 2-oxoglutaric acid. To test if ammonium affects GABA

337   transaminase activity, 30 mM $(NH_4)_2SO_4$ was added. The reaction mixture (initial volume 10

338   ml) was preincubated for 2 min at 30 °C and started by the addition of purified protein at a final

339   concentration of 3 µg mL^{-1}. Six 500 µl samples were collected over a period of 26 minutes and

340   the reaction was immediately terminated by mixing each sample with 300 µL of 5% (v/v)

341   perchloric acid and 38% (v/v) ethanol. After this, the sample was neutralized by addition of 200

342   µL of 20 mM Tris-HCl (pH 8) with 23 mM K_2CO_3. The precipitated salts were removed by

343   centrifugation (10 min, 16,000*g*). Subsequently, the glutamate concentration in the sample was

344 measured by HPLC (Agilent 1260 series) equipped with an Agilent Eclipse XDB-C18 column

345 using a variable wavelength detector and a fluorescence detector. Elution was performed with

346 a mixture of 43% (v/v) buffer A (10 mM Na_2HPO_4, 10 mM $Na_2B_4O_2$ (pH 8.2)) and 57% (v/v)

347 methanol at a flow rate of 2 mL/min for 14 minutes. Before chromatographic separation, amino

348 acids were derivatized with *o*-phthaldialdehyde (Lindroth and Mopper, 1979). 25-1000 μM

349 sodium glutamate was used as standard.

350

351 **RESULTS**

352 **Transcriptome comparison of WT cells grown with GABA or glucose**

353 To analyze the influence of GABA on global gene expression, we compared the transcriptomes

354 of cells cultivated in modified CGXII minimal medium lacking $(NH_4)_2SO_4$ and containing

355 either GABA or glucose as carbon source. In GABA-grown cells, 163 genes showed a ≥2-fold

356 increased mRNA level and 71 genes a ≥2-fold lowered mRNA level compared to glucose-

357 grown cells (Table S2). The genes showing the by far strongest upregulation in GABA-grown

358 cells were *gabTDP* (87-, 78-, and 65-fold, respectively) (Fig. 2 and Table S2). Interestingly,

359 also expression of the *gabR* gene located upstream and divergent to *gabTDP* was four-fold

360 increased in GABA-grown cells. The *gabR* gene encodes a transriptional regulator (see below).

361 Among the other genes upregulated in GABA-grown cells, only cg0083 encoding a putative

362 nicotinamide mononucleotide transporter showed a more than 10-fold increased expression. In

363 general, the upregulated genes belonged to a large variety of functional categories and the same

364 holds true for the genes downregulated in GABA-cultivated cells. The latter group included at

365 least 30 genes for proteins involved in transport, including those for phosphate uptake (*pitA,*

366 *pstSCAB*), genes involved in amino acid biosynthesis (*leuCD, serA, metE, argC, aroG, glnA*),

367 and genes involved in lactate metabolism (cg3226, *lldD*). In summary, this experiment

368 demonstrated that the *gabTDP* genes were strongly induced in the presence of GABA,

15

369   indicating that they are subject to transcriptional control. All other differentially expressed

370   genes were significantly less changed under this condition.

371

372   **Genomic location and conservation of the *gabR-gabTDP* gene cluster**

373   The *gabR* gene is located upstream and divergent to *gabTDP* and encodes a transcriptional

374   regulator, which might regulate these genes. To check whether this genomic organization is

375   conserved in related species, which is a hint for a regulatory relationship between these genes,

376   we analyzed the presence and organization of the *gabR-gabTDP* gene cluster in other

377   organisms. As shown in Fig. 3, similar gene clusters were found in a number of

378   *Corynebacterium* species and, in a different organization, also in some *Rhodococcus* and

379   *Mycobacterium* species. Interestingly, additional copies of *gabR* and *gabT* are present

380   immediately adjacent to the *gabR-gabTDP* gene cluster in *Corynebacterium aurimucosum*.

381   GabR and its homologs from *Actinobacteria* belong to the PucR protein family (Pfam PF07905)

382   and have a C-terminal DNA-binding HTH motif. The best characterized representative of this

383   family is PucR of *B. subtilis*, which is involved in the regulation of purine catabolism (Schultz

384   et al., 2001; Beier et al., 2002).

385

386   **Relevance of *gabR* and the *gabTDP* operon for growth with GABA**

387   To investigate whether GabR is involved in the regulation of GABA metabolism, we generated

388   the deletion mutant *C. glutamicum* Δ*gabR* and compared it with the WT. Both strains grew

389   identically with glucose, but the Δ*gabR* mutant had lost the ability to grow with GABA as sole

390   carbon and nitrogen source (Fig. 4a). The growth defect of the Δ*gabR* strain with GABA was

391   abolished after transformation with the expression plasmid pAN6-*gabR* harboring *gabR* under

392   control of a leaky *tac* promoter (Fig. 4b), which confirmed that the loss of GabR was responsible

393   for the observed phenotype. Whereas full complementation was achieved by basal *gabR*

394   expression in the absence of IPTG, induction of plasmid-borne *gabR* expression with 50 µM

395 IPTG had a negative effect on growth of the ΔgabR mutant and the WT in comparison to the

396 non-induced cultures (Fig. S1). This might be a consequence of too strong expression of the

397 gabTDP operon causing e.g. membrane-stress by overexpression of the permease-encoding

398 gene gabP or metabolic disturbances by an excessive GABA metabolism.

399   In a further experiment, we tested whether growth of the ΔgabR strain on GABA can be

400 restored by plasmid-based expression of gabTDP. C. glutamicum WT and the ΔgabR mutant

401 were transformed with pAN6-gabTDP and cultivated with GABA as sole carbon and nitrogen

402 source and different IPTG concentrations (Fig. 4c). Without IPTG addition, the ΔgabR strain

403 with pAN6-gabTDP grew very slowly. Addition of 10 µM IPTG significantly improved the

404 growth of this strain and with 100 µM IPTG it grew comparably to the WT carrying pAN6-

405 gabTDP. These results suggest that gabTDP are the only genes required for growth with GABA

406 that are controlled by GabR.

407

Purification of GabR and determination of the native size

409 The growth experiments with the ΔgabR mutant showed that GabR activates gabTDP

410 expression. To get further insights into the regulatory mechanism, we purified GabR for

411 interaction studies with the P_{gabTDP} promoter by EMSAs. GabR was overproduced in E. coli

412 BL21(DE3) and purified by means of an N-terminal decahistidine tag and Ni-NTA affinity

413 chromatography (Fig. 5a). The tag was cleaved off with TEV protease followed by size

414 exclusion chromatography to further purify GabR and determine its native size and oligomeric

415 state (Fig. 5b). The peak of GabR appeared at an elution volume of 10.67 mL. Based on the

416 calibration curve (K_{av} versus log M_r) derived from the standard proteins (Fig. 5c), the native

417 size of GabR was calculated to be 420 kDa. Since the theoretical mass of GabR is 55.75 kDa,

418 the native size suggests that C. glutamicum GabR forms an octamer (theoretical mass 446 kDa).

419

Determination of transcriptional start sites

In a previous RNAseq study, a TSS of P$_{gabR}$ was identified, but no TSS of P$_{gabTDP}$, presumably because the latter genes were not expressed in the absence of GABA (Pfeifer-Sancar et al., 2013). Therefore, we determined the TSS of P$_{gabTDP}$ initially using a 5′/3′-RACE kit and identified a single TSS for *gabT* located 36 bp upstream of the *gabT* start codon (Fig. 6a). The -10 region (TACTCA) and the -35 region (TTAACT) of P$_{gabTDP}$ and the RBS of *gabT* (AGGAG) were predicted according to known consensus sequences (Pfeifer-Sancar et al., 2013). In an alternative approach, we performed RNAseq of GABA-grown WT cells to identify TSSs. For *gabT*, the transcriptional start site found by 5′/3′-RACE was confirmed with 43906 reads starting at this position. Interestingly, another TSS was identified within the *gabD* coding region. 28 reads started 210 bp upstream of the *gabP* start codon, suggesting the presence of an additional weak promoter for *gabP* expression. The deduced -10 region (AACAAT) and -35 region (TTCGGC) showed reasonable similarity to the reported consensus sequences (Pfeifer-Sancar et al., 2013). This promoter might allow GabR-independent weak expression of *gabP* and could enable initial GABA uptake to allow GabR-dependent expression of the *gabTDP* operon. With respect to the TSS of *gabR*, the RNAseq data revealed only two reads that started at the position 59 bp upstream of the *gabR* start codon (Fig. 6a) that was previously reported (Pfeifer-Sancar et al., 2013). Four reads started 11 bp upstream of the *gabR* start codon, suggesting either another very weak promoter for *gabR* expression with weakly conserved -10 region (TAATTG) and -35 region (TTGTAG) or processing of the transcript starting 59 bp upstream of the *gabR* start codon.

Determination of the GabR binding site(s) in the *gabTDP* promoter region

For the determination of the GabR binding site, EMSAs were performed with purified GabR. In the first experiment, binding of GabR to a 500 bp fragment covering the entire *gabR-gabT* intergenic region was analyzed using a DNA fragment of similar size of the *ldhA* gene of *C*.

446 *glutamicum* as negative control. The *gabR-gabT* intergenic region was shifted partially with 80

447 nM GabR (monomer) and fully with 240 nM GabR (Fig. S2), whereas no shift was observed

448 for the control fragment up to 320 nM GabR (Fig. S2). This suggests that GabR binds

449 specifically to the *gabTDP* promoter region. In the following, we reduced the size of the DNA

450 fragments step by step to localize the binding site(s) of GabR using the above mentioned

451 fragments as positive and negative controls. As shown in Fig. S3, a full shift was observed for

452 fragments FA1 and FA2, a partial shift for FA3, and a very poor shift for FA4 and FA5. For the

453 fragments starting at the other side of the promoter region, clear shifts were observed for

454 fragments FB1, FB2 and FB3, weak shifts for FB4 and FB5, and no shift for FB6. These results

455 suggested that GabR binds between position -87 and -23 with respect to the TSS of *gabT*.

456   Regulator binding sites are often conserved among closely related species, which is useful

457 to identify a binding motif when only a single target promoter is known (Wennerhold et al.,

458 2005). We searched for a binding motif in the *gabR-gabT* intergenic regions of *C. glutamicum,*

459 *Corynebacterium deserti*, and *Corynebacterium callunae* using MEME software (Bailey et al.,

460 2006). The search uncovered a 21 bp inverted repeat that was present 1-2 times in each input

461 sequence (Fig. 6c). An alignment of the input sequences (Fig. S4) revealed that the regions

462 encompassing the two proposed GabR binding motifs belong to the more conserved regions,

463 which is a further hint that these represent GabR binding sites.

464   In further EMSAs, we used 55 bp fragments to verify the localization of the GabR binding

465 sites in the *C. glutamicum gabTDP* promoter. FS1 is a fragment covering both of the predicted

466 binding sites, whereas FS2 covers half of the first binding site and the entire second binding

467 site (Fig. 6a). A 55 bp fragment downstream of the predicted binding sites was used as negative

468 control. Binding of GabR was observed for both FS1 and FS2, but it was stronger for FS1 (Fig.

469 6b). This suggests that one complete binding site is sufficient for weak binding, but two sites

470 are required for strong binding by GabR. In another experiment, binding of GabR to two 31 bp

471 fragments (FS3 and FS4) covering one binding site each was tested. A 31 bp fragment

19

472 downstream of the predicted binding sites was used as negative control. Reasonable binding

473 was observed for FS3 containing the first binding site and weak binding, not much stronger

474 compared to the negative control, was observed for FS4 (Fig. S5). The band of the complex did

475 not run far into the gel, presumably because of the large size of the GabR octamer. We assume

476 that this band represents the complex, as it was absent from the negative control and from the

477 DNA samples without protein. Our results suggest that each of the two binding sites can be

478 bound separately by GabR, but binding is much stronger when both binding sites are present.

479 To verify that both binding sites are relevant for good binding, we mutated four conserved

480 bases of both motifs either separately or in combination in fragment FS1 and analyzed the

481 binding by GabR (Fig. S6). Mutation of one of the binding sites reduced the affinity to GabR,

482 and with both binding sites mutated, the binding was almost completely abolished. This verifies

483 that both sites are relevant for GabR binding.

484

485 **Influence of ammonium and urea on growth of *C. glutamicum* with GABA**

486 In our initial growth studies using the BioLector microcultivation system, *C. glutamicum* WT

487 was cultivated in standard CGXII minimal medium containing either glucose (41.7 mM

488 corresponding to 250 mM carbon) or GABA (62.5 mM corresponding to 250 mM carbon) as

489 carbon sources. In glucose-containing medium, a growth rate μ of 0.4 h^{-1} was observed, whereas

490 it was only 0.05 h^{-1} in GABA-containing medium. Interestingly, a growth rate of 0.13 h^{-1} was

491 obtained when the standard nitrogen sources of CGXII medium, ammonium sulfate (151 mM)

492 and urea (83 mM), were omitted and GABA served as sole carbon and nitrogen source (Fig.

493 7a). Measurement of the final OD$_{600}$ in a spectrophotometer after 50 h revealed no significant

494 difference between the cultures with glucose, $(NH_4)_2SO_4$ and urea on the one hand (OD$_{600}$ =

495 12.17 ± 0.54) and the cultures with GABA without additional nitrogen sources on the other

496 hand (OD$_{600}$ = 11.81 ± 0.96). Further growth experiments revealed that $(NH_4)_2SO_4$ alone was

497 sufficient to exert the same inhibitory effect on growth with GABA (μ = 0.04 h^{-1}) as in

498   combination with urea ($\mu = 0.05$ h^{-1}) (Fig. 7b). Urea alone was also inhibitory, but to a lesser

499   extent ($\mu = 0.08$ h^{-1}). Urea is converted by urease to ammonium and carbon dioxide (Siewe et

500   al., 1998), but the ammonia levels formed in this way are probably lower than in media

501   containing $(NH_4)_2SO_4$, which could explain the weaker inhibitory effect of urea. When similar

502   experiments were performed with glucose as carbon source, all cultures grew with the same

503   rate (Fig. 7c). A further experiment revealed that the inhibitory effect of $(NH_4)_2SO_4$ on growth

504   with GABA was concentration-dependent and weak inhibition was observed already with 10

505   mM $(NH_4)_2SO_4$ (Fig. S7). The negative influence of 151 mM $(NH_4)_2SO_4$ on the final backscatter

506   during growth with GABA as sole carbon source varied throughout our study. Sometimes the

507   same final backscatter was reached in the presence of $(NH_4)_2SO_4$ as in its absence, whereas in

508   other experiments the final backscatter was much lower in the presence of $(NH_4)_2SO_4$. The

509   reason for this variability is currently unknown. In summary, *C. glutamicum* grew quite well in

510   minimal medium with GABA as sole carbon and nitrogen source and the additional presence

511   of ammonium was inhibitory. In the following studies, we searched for the basis of ammonium

512   inhibition.

513

514   **Influence of ammonium on GABA consumption**

515   To test the influence of ammonium on GABA consumption, the WT was cultured in shake

516   flasks with minimal medium containing either GABA or GABA plus $(NH_4)_2SO_4$. With GABA

517   as sole carbon and nitrogen source, a growth rate of 0.12 h^{-1} was observed, which was reduced

518   to 0.08 h-1 in the presence of 151 mM $(NH_4)_2SO_4$ (Fig. 8a). In the absence of $(NH_4)_2SO_4$,

519   GABA (62.5 mM) was completely consumed after 24 h and only after about 36 h in the presence

520   of $(NH_4)_2SO_4$. Both cultures reached a final OD$_{600}$ of about 11, corresponding to 2.75 g cell dry

521   weight/L (Kabus et al., 2007). In a further experiment, cells were cultivated in minimal medium

522   containing either GABA and glucose or GABA, glucose, and $(NH_4)_2SO_4$. In this case, the

523   cultures with $(NH_4)_2SO_4$ grew slightly faster ($\mu = 0.46$ h^{-1}) than the ones without $(NH_4)_2SO_4$ (μ

524 = 0.39 h^{-1}) and also consumed glucose faster than the cultures without (NH$_4$)$_2$SO$_4$ (Fig. 8b).

525 Complete glucose consumption was observed after 8 h and 10 h, respectively. Interestingly,

526 GABA consumption was comparable for the cultures with and without (NH$_4$)$_2$SO$_4$, in contrast

527 to the cultures without glucose, and complete GABA consumption was observed after 12 h. It

528 is obvious from Fig. 8b that glucose and GABA are used simultaneously, also in the presence

529 of (NH$_4$)$_2$SO$_4$.

530

531 **Relevance of ammonia-assimilating enzymes for growth with GABA**

532 During growth in minimal medium with GABA as sole carbon and nitrogen source, L-glutamate

533 is formed from 2-oxoglutarate by the GABA transaminase GabT. L-Glutamine synthesis is

534 dependent on glutamine synthetase encoded by the *glnA* gene (Jakoby et al., 1997). A second

535 putative glutamine synthetase is encoded by *glnA2*, but this gene cannot complement the

536 glutamine auxotrophy of a Δ*glnA* mutant and the function of the GlnA2 protein is not known

537 yet (Nolden et al., 2001; Rehm and Burkovski, 2011). Glutamine synthetase requires L-

538 glutamate, ATP and NH$_4^+$ as substrates. Therefore, the question arises which reactions lead to

539 ammonia release and thereby allow glutamine synthesis during growth with GABA as sole

540 nitrogen source. A reasonable candidate is glutamate dehydrogenase (Gdh), which catalyzes

541 the reductive amination of 2-oxoglutarate with ammonia and NADPH to L-glutamate and

542 NADP$^+$, and also the reverse reaction (Shiio and Ozaki, 1970). In order to determine whether

543 Gdh is important as provider of ammonium during growth on GABA, we tested a Δ*gdh* mutant

544 and found that it grew similarly as the wild type with GABA as sole carbon and nitrogen source

545 (data not shown). This does not exclude the Gdh reaction as a source of ammonia, but shows

546 that alternative ways for ammonium generation exist.

547   Besides the Δ*gdh* mutant, we also tested the growth behavior on GABA of other mutants

548 with defects in nitrogen assimilation, which are mutants lacking either glutamate synthase

549 (Δ*gltBD*), or glutamine synthetase (Δ*glnA*), or a triple mutant devoid of GlnA, GlnA2, and Gdh

22

550   ($\Delta glnA\Delta glnA2\Delta gdh$). Whereas the $\Delta gltBD$ mutant grew like the WT, the other two mutants

551   were unable to grow with GABA as sole carbon and nitrogen source, irrespective of the absence

552   or presence of ammonium. In Fig. 9, the data for the triple mutant are shown. The result

553   corresponds to the expectation that GltBD is not required for glutamate synthesis, whereas

554   GlnA is essential for glutamine synthesis. This was further confirmed by supplementing GABA

555   medium with L-glutamine, which rescued growth of the triple mutant (Fig. 9). The addition of

556   L-glutamine also improved the growth rate of the WT with GABA by about 50% ($\mu = 0.15$ h^{-1}

557   vs. $\mu = 0.10$ h^{-1} without glutamine) and the final backscatter by about 25% (Fig. 9). *C.*

558   *glutamicum* is able to use L-glutamine as sole carbon and nitrogen source (Rehm et al., 2010).

559   Whereas the increased final backscatter can be explained by the use of L-glutamine as

560   additional carbon source, the increased growth rate suggests a deficiency in glutamine

561   availability when GABA serves as sole nitrogen source. Interestingly, when $(NH_4)_2SO_4$ was

562   added to medium with GABA and glutamine, it again had a negative effect on growth of both

563   the WT and the triple mutant (Fig. 9). This suggests that the inhibitory effect of ammonium on

564   growth with GABA alone is not due to a negative effect on glutamine synthesis.

565

566   **Influence of growth conditions and GabR on the promoter activity of P$_{gabTDP}$**

567   To analyze the influence of ammonia and other conditions on the expression of the *gabTDP*

568   operon, we constructed the reporter plasmid pJC1-P$_{gabT}$-eYFP containing a transcriptional

569   fusion between P$_{gabTDP}$ (500 bp upstream of the *gabT* start codon) and the eYFP-encoding gene.

570   Thereby the promoter activity can be monitored by measuring the fluorescence of the culture.

571   Cell density (backscatter) and eYFP fluorescence of WT cells with pJC1-P$_{gabT}$-eYFP cultivated

572   in different media is shown in Fig. 10a,b. As the cells reached different final backscatter values,

573   the specific fluorescence (representing the ratio of fluorescence/backscatter) was calculated for

574   the cultures in the stationary phase at 40 h, which represents the activity of P$_{gabTDP}$ over the

575   entire cultivation (Fig. 10c). We also checked the specific fluorescence of the cultures in the

576 exponential growth phase, which were very similar to the values after 40 h (data not shown).

577 Maximal specific fluorescence (2.81 ± 0.07) was observed for the cultures grown with GABA

578 alone, whereas it was almost zero (0.03 ± 0.00) for the cultures grown with glucose alone,

579 indicating that P$_{gabTDP}$ was active only in the presence of GABA. The specific fluorescence of

580 the cultures grown with GABA, ammonium sulfate and urea (1.84 ± 0.10) was reduced by 35%

581 in comparison to the cultures with GABA alone, indicating that ammonium inhibited

582 transcription of *gabTDP*. Addition of glutamine to a culture with GABA and ammonium sulfate

583 did not enhance *gabTDP* expression (data not shown), suggesting that glutamine does not

584 influence transcription of *gabTDP*.

585   The specific fluorescence of cells cultivated with GABA, glucose, ammonium sulfate and

586 urea (0.90 ± 0.02) was reduced by even 68% compared to growth on GABA alone, indicating

587 that not only ammonium, but also glucose had a negative effect on *gabTDP* transcription. This

588 effect was not specific for glucose, as it was also observed with gluconate or *myo*-inositol as

589 additional carbon sources (Fig. S8).

590   In further experiments, we analyzed the activity of P$_{gabTDP}$ in the Δ*gabR* mutant (Fig. 10d

591 and 10e). In medium with only GABA as carbon and nitrogen source, the mutant showed

592 neither growth nor fluorescence, as expected. In medium with glucose and GABA, the mutant

593 was able to grow, but no fluorescence was observed. This result confirms that besides GABA

594 also GabR is essential for expression of the *gabTDP* genes.

595

596 **Influence of plasmid-based *gabTDP* expression on the effect of ammonium**

597 The reporter gene assays had revealed that ammonium reduces transcription of *gabTDP* (Fig.

598 10c) by about 35%. To test whether this effect is sufficient to explain the growth inhibition by

599 ammonium, we analyzed the consequences of plasmid-based overexpression of *gabTDP*. *C.*

600 *glutamicum* WT was transformed with pAN6-*gabTDP* or pAN6 as control. The two strains

601 were cultivated with GABA alone or with GABA plus $(NH_4)_2SO_4$ and expression of plasmid-

24

602 borne *gabTDP* was induced with 10 µM IPTG (Fig. 11). With GABA alone, the WT containing

603 pAN6-*gabTDP* grew comparably to the control strain with pAN6, suggesting that under these

604 conditions chromosomal *gabTDP* expression was not limiting growth. In medium with GABA

605 and $(NH_4)_2SO_4$, the strain with pAN6-*gabTDP* grew faster than the control strain with pAN6,

606 although still not as good as with GABA alone, even when *gabTDP* expression was induced

607 with 100 µM IPTG (data not shown). The results indicate that increased expression of *gabTDP*

608 can partially overcome the growth inhibition by $(NH_4)_2SO_4$.

609

610 **DISCUSSION**

611 In this study, we analyzed the regulation of GABA utilization in the actinobacterial model

612 organism *C. glutamicum*. The fact that *C. glutamicum* possesses the genes/proteins required for

613 GABA uptake and metabolism suggests that GABA occurs in its natural soil habitat, where it

614 could be derived e.g. from decomposed plant material or formed by other microorganisms via

615 glutamate decarboxylation. We show that expression of the *gabTDP* operon encoding the

616 proteins involved in GABA uptake and catabolism is transcriptionally activated by the

617 divergently encoded regulator GabR. GabR is essential for growth of *C. glutamicum* on GABA.

618 The observation that growth of a Δ*gabR* mutant could be restored by plasmid-based, GabR-

619 independent expression of the *gabTDP* genes indicated that no additional genes activated by

620 GabR are required for GABA utilization, characterizing GabR as a local regulator.

621   GabR belongs to the PucR family of transcriptional regulators (Pfam PF07905). According

622 to Pfam, more than 95% of the PucR sequences in the database are derived from *Actinobacteria*

623 or *Firmicutes*. About half of the PucR family members in the database contain a GGDEF-like

624 domain. Only few PucR-type regulators were studied to date, all of which contain the GGDEF-

625 like domain, but a specific function of this domain has not been reported. These regulators are

626 *B. subtilis* PucR involved in purine catabolism (Beier et al., 2002), *B. subtilis* PutR involved in

627 proline utilization (Belitsky, 2011), *B. subtilis* AdeR involved in alanine catabolism (Lin et al.,

2012), *Streptomyces ambofaciens* Srm22 (SrmR) controlling expression of a polyketide synthase gene for the synthesis of an antibiotic (Geistlich et al., 1992; Karray et al., 2010), and *Escherichia coli* CdaR (SdaR), which regulates genes involved in the uptake and metabolism of galactarate and glucarate (Monterrubio et al., 2000). All of these PucR regulators are activators, except for *B. subtilis* PucR, which acts both as activator and as repressor. GabR from *C. glutamicum* is the first characterized member of the PucR family that does not contain a GGDEF-like domain. Our results suggest that GabR binds to two 21 bp inverted repeats in the *gabTDP* promoter region. For AdeR, a 24 bp inverted repeat and for PutR, a 17 bp inverted repeat have been determined as binding sites, which is similar to our findings (Belitsky, 2011; Lin et al., 2012). The binding site of PucR is not palindromic (Beier et al., 2002) and the binding sites for Srm22 and CdaR have not been determined yet.

Gel filtration of GabR indicated that it forms octamers. As the oligomeric state of other PucR-like regulators has not been determined yet, we do not know whether this is a specific feature of this group of regulators. We searched for other octameric transcriptional regulators to compare their binding patterns and function. The LysR-type transcriptional regulator (LTTR) CrgA of *Neisseria meningitides* forms octameric rings and is proposed to bind to two binding sites in its target promoter with two stacked octameric rings (Sainsbury et al., 2009). The two CrgA binding sites cover a region of 63 bp, which is quite similar in size to the region covered by our two proposed motifs. CrgA also binds to DNA fragments containing just one of the binding sites (Sainsbury et al., 2009), but with strongly decreased affinity, which is also comparable to our data. GabR might work in a similar manner. Regulators belonging to the Lrp family are also frequently forming octamers, for example Lrp of *E. coli* (de los Rios and Perona, 2007), LrpA of *Pyrococcus furiosus* (Leonard et al., 2001), LrpA of *Mycobacterium tuberculosis* (Reddy et al., 2008; Song et al., 2016), AldR of *M. tuberculosis* (Dey et al., 2016), or BarR of the archeum *Sulfolobus acidocaldarius* (Liu et al., 2014).

26

653   Transcriptional activators for catabolic pathways often require the corresponding substrate

654   or one of its degradation products as co-activator. In the case of GabR from *C. glutamicum*,

655   binding to its target DNA did not require the presence of GABA and the presence of GABA

656   had no obvious influence on the binding affinity (Fig. S9). GabR might bind to its target DNA

657   both in the apo-state and in the ligand-bound state, but requires binding of GABA or another

658   effector metabolite to trigger a conformational change that is necessary to activate transcription

659   of *gabTDP*. Such a situation was found e.g. for *B. subtilis* GabR$_{Bs}$, which binds to its target

660   promoter independent of GABA, but transcription activation of the target genes requires

661   binding of GABA and PLP (Wu et al., 2017). However, GabR$_{Bs}$ belongs to a different protein

662   family than GabR of *C. glutamicum* and also PLP had no influence on GabR binding to DNA,

663   neither alone nor in combination with GABA (Fig. S9). In case of *B. subtilis* PutR, the presence

664   of proline increased the affinity for its target DNA about 10-fold (Belitsky, 2011), whereas for

665   *B. subtilis* AdeR, L-alanine did not increase the affinity for the target promoter (Lin et al., 2012).

666   Further studies are required to identify the co-activator(s) of GabR and the mechanism of

667   transcriptional activation.

668   The GabR binding site is located immediately upstream of the -35 region of P$_{gabTDP}$ (Fig.

669   6), which is a typical position for transcriptional activators. However, in the transcriptome

670   analysis, not only the *gabTDP* mRNA levels were increased during growth with GABA, but

671   also the *gabR* mRNA level, although to a much lesser extent (4-fold) compared to *gabTDP* (65-

672   to 87-fold). As the GabR binding site is located downstream of the -10 region of the *gabR*

673   promoter identified in previous RNAseq studies (Pfeifer-Sancar et al., 2013), the question arises

674   how the apparent positive autoregulation of *gabR* is accomplished. One possibility could be an

675   alternative transcriptional start site, leading e.g. to a leaderless transcript, which is found quite

676   often in *C. glutamicum*. Our RNAseq analysis indeed identified a possible alternative TSS

677   located 11 bp upstream of the *gabR* start codon (Fig. 6a), but also in this case the promoter

678   region overlaps with one of the two GabR binding sites.

When GABA is used as sole carbon source by *C. glutamicum*, growth requires the formation of PEP for gluconeogenesis. This task is fulfilled by PEP carboxykinase encoded by the *pck* gene (Riedel et al., 2001). Expression of the *pck* gene was found to be slighly upregulated in cells grown with GABA (1.68-fold, p-value 0.02), supporting its requirement in gluconeogenesis. Transcription of *pck* is subject to regulation by at least four transcriptional regulator and upregulation during growth on GABA might be due to derepression by RamA or activation by GntR1/GntR2 (Klaffl et al., 2013).

We observed that ammonium inhibits growth with GABA, with 10 mM already showing slight growth retardation. This negative effect is caused at least in part by an influence on *gabTDP* transcription, which was reduced by about 35% in the presence of 151 mM ammonium and 83 mM urea (Fig. 10). The molecular basis for the diminished expression is not known yet. Control of nitrogen metabolism has been extensively studied in *C. glutamicum* and AmtR was identified as global regulator (Jakoby et al., 2000; Beckers et al., 2005; Buchinger et al., 2009). In the presence of sufficient nitrogen, AmtR represses a large set of genes involved in uptake and utilization of various nitrogen sources. However, the *gabTDP* operon or *gabR* were never identified as members of the AmtR regulon, arguing against AmtR as mediator of reduced *gabTDP* expression in the presence of ammonia. In our EMSA studies with purified GabR, ammonia did not influence binding to the *gabT* promoter region (Fig. S10), but this does not exclude an effect of ammonia on GabR-activated transcription initiation. For example, binding of ammonium to GabR might inhibit binding of GABA or another effector and thus transcriptional activation. Future studies are required to clarify the mechanism by which ammonium inhibits *gabTDP* expression.

Growth with GABA as sole carbon and nitrogen sources requires the formation of ammonium as substrate for glutamine synthetase. Oxidative deamination of glutamate by glutamate dehydrogenase might contribute to ammonium provision, although deletion of the *gdh* gene had no effect on growth with GABA. An alternative possibility is the reaction

catalyzed by aspartate ammonia-lyase, which catalyzes the conversion of aspartate to fumarate and ammonia (Dover and Halpern, 1972). The corresponding gene *aspA* (cg1697) was 2.50-fold upregulated in cells grown with GABA and urea compared to cells grown with glucose and urea. The observation that glutamine supplementation improved the growth rate with GABA suggests that glutamine availability in the absence of supplementation is limited, presumably by limited availability of the ammonia for glutamine synthetase. However, glutamine stimulated growth also in the presence of ammonium. In this situation, glutamine synthetase activity might be limiting due to limited expression of the *glnA* gene in the presence of ammonium (Nolden et al., 2001; Strösser et al., 2004) and due to limited activity of the enzyme due to adenylylation by GlnE (Amon et al., 2010; Rehm and Burkovski, 2011). We also tested whether ammonium inhibits the activity of the GabT transaminase activity using purified GabT, but observed only a slight reduction by 6% in the presence of 30 mM $(NH_4)_2SO_4$ (9.07 ± 0.33 µmol min^{-1} mg^{-1} vs. 9.69 ± 0.12 µmol min^{-1} mg^{-1} in the absence of ammonium sulfate).

Besides ammonium, also the presence of alternative carbon sources had a negative influence on the expression of the *gabTDP* operon. The inhibition by glucose, gluconate, and *myo*-inositol is presumably caused by repression of *gabTDP* by the global cAMP-dependent transcriptional regulator GlxR. GlxR can function both as activator and repressor, depending on the localization of the binding site. A GlxR binding site (5'-TGTATCTCACCTCACA-3') has been detected in the *gabR-gabT* intergenic region (Toyoda et al., 2011; Jungwirth et al., 2013), which is located downstream of the *gabT* TSS (Fig. 6a), indicating a repressor function of GlxR for *gabTDP*. GlxR-binding to DNA is controlled by cAMP, which is formed by the membrane-bound adenylate cyclase CyaB (Cha et al., 2010; Wolf et al., 2020). The tested additional carbon sources might lead to elevated cAMP levels and thus to enhanced binding of GlxR to the *gabT* promoter and repression. In contrast to e.g. *E. coli*, *C. glutamicum* usually shows parallel consumption of carbon sources rather than diauxic growth. This has been

demonstrated e.g. for glucose and acetate (Wendisch et al., 2000), glucose and gluconate (Frunzke et al., 2008), or glucose and citrate (Brocker et al., 2009). GlxR is presumably involved in coordinating the consumption of carbon sources in *C. glutamicum* to avoid an overload of the metabolic capacity of the cells. In the case of GABA, a similar situation can be envisaged, where the presence of an alternative carbon source causes a reduction of the GABA utilization rate to avoid an overload of the TCA cycle at the stage of succinate.

In summary, we characterized GabR as the first PucR-type transcriptional regulator without a GGDEF-like domain and showed that GabR is essential for activating expression of the GABA catabolic genes *gabTDP*. Although GABA did not influence the binding affinity of purified GabR to its target promoter, we assume it to be the most likely effector molecule, as the *gabTDP* genes were not expressed in the absence of GABA. The inhibitory effect of ammonium on GABA utilization is caused via inhibition of *gabTDP* transcription via a yet unknown mechanism and presumably via a negative effect on glutamine synthetase expression and activity. The negative effect on *gabTDP* transcription by alternative carbon sources is likely caused by the global cAMP-dependent regulator GlxR. Many of the results obtained here will probably also be relevant for other *Actinobacteria* capable of utilizing GABA as carbon and nitrogen source.

DATA AVAILABILITY STATEMENT

This manuscript contains previously unpublished data. The DNA microarray data are available in the GEO database with the accession number GSE138829. The RNAseq data are available in the GEO database with the accession number GSE156688.

AUTHOR CONTRIBUTIONS

LZ performed the majority of the experimental work presented in this study. CM performed several growth experiments in shake flasks and the BioLector microcultivation system and she

30

performed the RNA isolation for RNAseq analysis. AW established and performed the HPLC

method for measuring the GABA concentration in supernatants. AK evaluated the RNAseq data

and TP supported the DNA microarray analysis. MBa and MBo designed the study, supervised

the experimental work, and evaluated the data together with LZ, AK, and TP. LZ wrote the first

draft of the manuscript and provided most of the figures and tables. MBa prepared figures added

during revision. MBa and MBo revised the manuscript and MBo was responsible for the final

version.

SUPPLEMENTARY MATERIAL

Tables S1 and S2

Figures S1 – S10

REFERENCES

Abdou, A.M., Higashiguchi, S., Horie, K., Kim, M., Hatta, H., and Yokogoshi, H. (2006). Relaxation and immunity enhancement effects of γ-aminobutyric acid (GABA) administration in humans. *BioFactors* 26(3), 201-208. doi: 10.1002/biof.5520260305.

Amon, J., Titgemeyer, F., and Burkovski, A. (2010). Common patterns - unique features: nitrogen metabolism and regulation in Gram-positive bacteria. *FEMS Microbiol. Rev.* 34(4), 588-605. doi: 10.1111/j.1574-6976.2010.00216.x.

Bailey, T.L., Williams, N., Misleh, C., and Li, W.W. (2006). MEME: discovering and analyzing DNA and protein sequence motifs. *Nucleic Acids Res.* 34, W369-373. doi: 10.1093/nar/gkl198.

Baumgart, M., Luder, K., Grover, S., Gätgens, C., Besra, G.S., and Frunzke, J. (2013). IpsA, a novel LacI-type regulator, is required for inositol-derived lipid formation in *Corynebacteria* and *Mycobacteria*. *BMC Biol.* 11, 122. doi: 10.1186/1741-7007-11-122.

Beckers, G., Strösser, J., Hildebrandt, U., Kalinowski, J., Farwick, M., Krämer, R., et al. (2005). Regulation of AmtR-controlled gene expression in *Corynebacterium glutamicum*: mechanism and characterization of the AmtR regulon. *Mol. Microbiol.* 58(2), 580-595.

Beier, L., Nygaard, P., Jarmer, H., and Saxild, H.H. (2002). Transcription analysis of the *Bacillus subtilis* PucR regulon and identification of a cis-acting sequence required for PucR-regulated expression of genes involved in purine catabolism. *J. Bacteriol.* 184(12), 3232-3241. doi: 10.1128/jb.184.12.3232-3241.2002.

Belitsky, B.R. (2004). *Bacillus subtilis* GabR, a protein with DNA-binding and aminotransferase domains, is a PLP-dependent transcriptional regulator. *J. Mol. Biol.* 340(4), 655-664. doi: 10.1016/j.jmb.2004.05.020.

Belitsky, B.R. (2011). Indirect repression by *Bacillus subtilis* CodY *via* displacement of the activator of the proline utilization operon. *J. Mol. Biol.* 413(2), 321-336. doi: 10.1016/j.jmb.2011.08.003.

Ben-Ari, Y., Gaiarsa, J.L., Tyzio, R., and Khazipov, R. (2007). GABA: a pioneer transmitter that excites immature neurons and generates primitive oscillations. *Physiol. Rev.* 87(4), 1215-1284. doi: 10.1152/physrev.00017.2006.

Bertani, G. (1951). Studies on lysogenesis. I. The mode of phage liberation by lysogenic *Escherichia coli*. *J. Bacteriol.* 62(3), 293-300.

Brocker, M., Schaffer, S., Mack, C., and Bott, M. (2009). Citrate utilization by *Corynebacterium glutamicum* is controlled by the CitAB two-component system through positive regulation of the citrate transport genes *citH* and *tctCBA*. *J. Bacteriol.* 191(12), 3869-3880. doi: 10.1128/jb.00113-09.

Buchinger, S., Strösser, J., Rehm, N., Hänssler, E., Hans, S., Bathe, B., et al. (2009). A combination of metabolome and transcriptome analyses reveals new targets of the *Corynebacterium glutamicum* nitrogen regulator AmtR. *J. Biotechnol.* 140, 68-74.

Bussmann, M., Baumgart, M., and Bott, M. (2010). RosR (Cg1324), a hydrogen peroxide-sensitive MarR-type transcriptional regulator of *Corynebacterium glutamicum*. *J. Biol. Chem.* 285(38), 29305-29318. doi: 10.1074/jbc.M110.156372.

Cha, P.H., Park, S.Y., Moon, M.W., Subhadra, B., Oh, T.K., Kim, E., et al. (2010). Characterization of an adenylate cyclase gene (*cyaB*) deletion mutant of *Corynebacterium glutamicum* ATCC 13032. *Appl. Microbiol. Biotechnol.* 85, 1061-1068.

Cotter, P.D., and Hill, C. (2003). Surviving the acid test: Responses of gram-positive bacteria to low pH. *Microbiol. Mol. Biol. Rev.* 67(3), 429-453. doi: Doi 10.1128/Mmbr.37.3.429-453.2003.

De Biase, D., and Pennacchietti, E. (2012). Glutamate decarboxylase-dependent acid resistance in orally acquired bacteria: function, distribution and biomedical implications of the *gadBC* operon. *Mol. Microbiol.* 86, 770-786. doi: 10.1111/mmi.12020.

de los Rios, S., and Perona, J.J. (2007). Structure of the *Escherichia coli* leucine-responsive regulatory protein Lrp reveals a novel octameric assembly. *J. Mol. Biol.* 366(5), 1589-1602. doi: 10.1016/j.jmb.2006.12.032.

Dey, A., Shree, S., Pandey, S.K., Tripathi, R.P., and Ramachandran, R. (2016). Crystal structure of *Mycobacterium tuberculosis* H37Rv AldR (Rv2779c), a regulator of the *ald* Gene: DNA binding and identification of small molecule inhibitors *J. Biol. Chem.* 291(23), 11967-11980. doi: 10.1074/jbc.M115.700484.

833 Dhakal, R., Bajpai, V.K., and Baek, K.H. (2012). Production of GABA (γ-aminobutyric acid) by
834   microorganisms: a review. *Braz. J. Microbiol.* 43(4)**,** 1230-1241. doi: 10.1590/S1517-
835   83822012000400001.

836 Dover, S., and Halpern, Y.S. (1972). Utilization of γ-aminobutyric acid as the sole carbon and nitrogen
837   source by *Escherichia coli* K-12 mutants. *J. Bacteriol.* 109(2)**,** 835-843.

838 Edayathumangalam, R., Wu, R., Garcia, R., Wang, Y., Wang, W., Kreinbring, C.A., et al. (2013).
839   Crystal structure of *Bacillus subtilis* GabR, an autorepressor and transcriptional activator of
840   gabT. *Proc. Natl. Acad. Sci. USA* 110(44)**,** 17820-17825. doi: 10.1073/pnas.1315887110.

841 Eggeling, L., and Bott, M. (eds.). (2005). *Handbook of Corynebacterium glutamicum.* Boca Raton,
842   Florida, USA: CRC Press, Taylor & Francis Group.

843 Ewing, B., and Green, P. (1998). Base-calling of automated sequencer traces using phred. II. Error
844   probabilities. *Genome Res.* 8(3)**,** 186-194.

845 Feehily, C., and Karatzas, K.A. (2013). Role of glutamate metabolism in bacterial responses towards
846   acid and other stresses. *J. Appl. Microbiol.* 114(1)**,** 11-24. doi: 10.1111/j.1365-
847   2672.2012.05434.x.

848 Foster, J.W. (2004). Escherichia coli acid resistance: tales of an amateur acidophile. *Nat. Rev. Microbiol.*
849   2(11)**,** 898-907. doi: 10.1038/nrmicro1021.

850 Frunzke, J., Engels, V., Hasenbein, S., Gätgens, C., and Bott, M. (2008). Co-ordinated regulation of
851   gluconate catabolism and glucose uptake in *Corynebacterium glutamicum* by two functionally
852   equivalent transcriptional regulators, GntR1 and GntR2. *Mol. Microbiol.* 67(2)**,** 305-322.

853 Geistlich, M., Losick, R., Turner, J.R., and Rao, R.N. (1992). Characterization of a novel regulatory
854   gene governing the expression of a polyketide synthase gene in *Streptomyces ambofaciens*. *Mol.*
855   *Microbiol.* 6(14)**,** 2019-2029. doi: 10.1111/j.1365-2958.1992.tb01374.x.

856 Gibson, D.G., Young, L., Chuang, R.Y., Venter, J.C., Hutchison, C.A., and Smith, H.O. (2009).
857   Enzymatic assembly of DNA molecules up to several hundred kilobases. *Nat. Meth.* 6(5)**,** 343-
858   345. doi: 10.1038/Nmeth.1318.

859 Hanahan, D. (1983). Studies on transformation of *Escherichia coli* with plasmids. *J. Mol. Biol.* 166(4)**,**
860   557-580.

861 Hilker, R., Stadermann, K.B., Doppmeier, D., Kalinowski, J., Stoye, J., Straube, J., et al. (2014).
862   ReadXplorer--visualization and analysis of mapped sequences. *Bioinformatics* 30(16)**,** 2247-
863   2254. doi: 10.1093/bioinformatics/btu205.

864 Hong, J., and Kim, K.J. (2019). Crystal structure of γ-aminobutyrate aminotransferase in complex with
865   a PLP-GABA adduct from *Corynebacterium glutamicum*. *Biochem. Biophys. Res. Commun.*
866   514(3)**,** 601-606. doi: 10.1016/j.bbrc.2019.04.194.

867 Jakoby, M., Nolden, L., Meier-Wagner, J., Krämer, R., and Burkovski, A. (2000). AmtR, a global
868   repressor in the nitrogen regulation system of *Corynebacterium glutamicum*. *Mol. Microbiol.*
869   37(4)**,** 964-977.

870 Jakoby, M., Tesch, M., Sahm, H., Krämer, R., and Burkovski, A. (1997). Isolation of the
871   *Corynebacterium glutamicum glnA* gene encoding glutamine synthetase I. *FEMS Microbiol.*
872   *Lett.* 154(1)**,** 81-88.

873 Jorge, J.M., Leggewie, C., and Wendisch, V.F. (2016). A new metabolic route for the production of
874   gamma-aminobutyric acid by *Corynebacterium glutamicum* from glucose. *Amino Acids* 48(11)**,**
875   2519-2531. doi: 10.1007/s00726-016-2272-6.

876 Jungwirth, B., Sala, C., Kohl, T.A., Uplekar, S., Baumbach, J., Cole, S.T., et al. (2013). High-resolution
877   detection of DNA binding sites of the global transcriptional regulator GlxR in *Corynebacterium*
878   *glutamicum*. *Microbiology* 159**,** 12-22. doi: 10.1099/mic.0.062059-0.

879 Kabus, A., Niebisch, A., and Bott, M. (2007). Role of cytochrome *bd* oxidase from *Corynebacterium*
880   *glutamicum* in growth and lysine production. *Appl. Environ. Microbiol.* 73**,** 861-868.

881 Kalinowski, J., Bathe, B., Bartels, D., Bischoff, N., Bott, M., Burkovski, A., et al. (2003). The complete
882   *Corynebacterium glutamicum* ATCC 13032 genome sequence and its impact on the production
883   of L-aspartate-derived amino acids and vitamins. *J. Biotechnol.* 104(1-3)**,** 5-25.

884 Kapust, R.B., and Waugh, D.S. (1999). *Escherichia coli* maltose-binding protein is uncommonly
885   effective at promoting the solubility of polypeptides to which it is fused. *Protein Sci.* 8**,** 1668-
886   1674. doi: 10.1110/ps.8.8.1668.

Karray, F., Darbon, E., Nguyen, H.C., Gagnat, J., and Pernodet, J.L. (2010). Regulation of the biosynthesis of the macrolide antibiotic spiramycin in *Streptomyces ambofaciens*. *J. Bacteriol.* 192(21), 5813-5821. doi: 10.1128/JB.00712-10.

Kawasaki, N., Nakayama, A., Yamano, N., Takeda, S., Kawata, Y., Yamamoto, N., et al. (2005). Synthesis, thermal and mechanical properties and biodegradation of branched polyamide 4. *Polymer* 46(23), 9987-9993. doi: 10.1016/j.polymer.2005.06.092.

Keilhauer, C., Eggeling, L., and Sahm, H. (1993). Isoleucine synthesis in *Corynebacterium glutamicum*: molecular analysis of the *ilvB-ilvN-ilvC* operon. *J. Bacteriol.* 175(17), 5595-5603.

Kensy, F., Engelbrecht, C., and Büchs, J. (2009a). Scale-up from microtiter plate to laboratory fermenter: evaluation by online monitoring techniques of growth and protein expression in *Escherichia coli* and *Hansenula polymorpha* fermentations. *Microb. Cell Fact.* 8, 68. doi: 10.1186/1475-2859-8-68.

Kensy, F., Zang, E., Faulhammer, C., Tan, R.K., and Büchs, J. (2009b). Validation of a high-throughput fermentation system based on online monitoring of biomass and fluorescence in continuously shaken microtiter plates. *Microb. Cell Fact.* 8, 31. doi: 10.1186/1475-2859-8-31.

Kinoshita, S., Udaka, S., and Shimono, M. (1957). Studies on amino acid fermentation. Part I. Production of L-glutamic acid by various microorganisms. *J. Gen. Appl. Microbiol.* 3, 193-205.

Klaffl, S., Brocker, M., Kalinowski, J., Eikmanns, B.J., and Bott, M. (2013). Complex regulation of the phosphoenolpyruvate carboxykinase gene *pck* and characterization of its GntR-Type regulator IolR as a repressor of *myo*-inositol utilization genes in *Corynebacterium glutamicum*. *J. Bacteriol.* 195(18), 4283-4296. doi: 10.1128/JB.00265-13.

Kortmann, M., Kuhl, V., Klaffl, S., and Bott, M. (2015). A chromosomally encoded T7 RNA polymerase-dependent gene expression system for *Corynebacterium glutamicum*: construction and comparative evaluation at the single-cell level. *Microb. Biotechnol.* 8(2), 253-265. doi: 10.1111/1751-7915.12236.

Krulwich, T.A., Sachs, G., and Padan, E. (2011). Molecular aspects of bacterial pH sensing and homeostasis. *Nat. Rev. Microbiol.* 9(5), 330-343. doi: 10.1038/nrmicro2549.

Kurihara, S., Kato, K., Asada, K., Kumagai, H., and Suzuki, H. (2010). A putrescine-inducible pathway comprising PuuE-YneI in which γ-aminobutyrate is degraded into succinate in *Escherichia coli* K-12. *J. Bacteriol.* 192(18), 4582-4591. doi: 10.1128/JB.00308-10.

Leonard, P.M., Smits, S.H., Sedelnikova, S.E., Brinkman, A.B., de Vos, W.M., van der Oost, J., et al. (2001). Crystal structure of the Lrp-like transcriptional regulator from the archaeon *Pyrococcus furiosus*. *EMBO J.* 20(5), 990-997. doi: 10.1093/emboj/20.5.990.

Lin, T.H., Wei, G.T., Su, C.C., and Shaw, G.C. (2012). AdeR, a PucR-type transcription factor, activates expression of L-alanine dehydrogenase and is required for sporulation of *Bacillus subtilis*. *J. Bacteriol.* 194(18), 4995-5001. doi: 10.1128/JB.00778-12.

Lindroth, P., and Mopper, K. (1979). High-Performance liquid chromatographic determination of subpicomole amounts of amino acids by precolumn fluorescence derivatization with *o*-phthaldialdehyde. *Anal. Chem.* 51(11), 1667-1674.

Liu, H., Orell, A., Maes, D., van Wolferen, M., Lindas, A.C., Bernander, R., et al. (2014). BarR, an Lrp-type transcription factor in *Sulfolobus acidocaldarius*, regulates an aminotransferase gene in a β-alanine responsive manner. *Mol. Microbiol.* 92(3), 625-639. doi: 10.1111/mmi.12583.

Marienhagen, J., Kennerknecht, N., Sahm, H., and Eggeling, L. (2005). Functional analysis of all aminotransferase proteins inferred from the genome sequence of *Corynebacterium glutamicum*. *J. Bacteriol.* 187(22), 7639-7646.

Medema, M.H., Takano, E., and Breitling, R. (2013). Detecting sequence homology at the gene cluster level with MultiGeneBlast. *Mol. Biol. Evol.* 30(5), 1218-1223. doi: 10.1093/molbev/mst025.

Michaeli, S., and Fromm, H. (2015). Closing the loop on the GABA shunt in plants: are GABA metabolism and signaling entwined? *Front. Plant Sci.* 6, 419. doi: 10.3389/fpls.2015.00419.

Monterrubio, R., Baldoma, L., Obradors, N., Aguilar, J., and Badia, J. (2000). A common regulator for the operons encoding the enzymes involved in D-galactarate, D-glucarate, and D-glycerate utilization in *Escherichia coli*. *J. Bacteriol.* 182(9), 2672-2764. doi: 10.1128/jb.182.9.2672-2674.2000.

Müller, T., Strösser, J., Buchinger, S., Nolden, L., Wirtz, A., Krämer, R., et al. (2006). Mutation-induced metabolite pool alterations in *Corynebacterium glutamicum*: towards the identification of nitrogen control signals. *J. Biotechnol.* 126(4)**,** 440-453. doi: 10.1016/j.jbiotec.2006.05.015.

Ni, Y., Shi, F., and Wang, N. (2015). Specific γ-aminobutyric acid decomposition by *gabP* and *gabT* under neutral pH in recombinant *Corynebacterium glutamicum. Biotechnol. Lett.* 37(11)**,** 2219-2227. doi: 10.1007/s10529-015-1897-y.

Niebisch, A., and Bott, M. (2001). Molecular analysis of the cytochrome bc_1-aa_3 branch of the *Corynebacterium glutamicum* respiratory chain containing an unusual diheme cytochrome c_1. *Arch. Microbiol.* 175(4)**,** 282-294.

Nolden, L., Farwick, M., Krämer, R., and Burkovski, A. (2001). Glutamine synthetases of *Corynebacterium glutamicum*: transcriptional control and regulation of activity. *FEMS Microbiol. Lett.* 201**,** 91-98.

Peng, Q., Yang, M., Wang, W., Han, L., Wang, G., Wang, P., et al. (2014). Activation of *gab* cluster transcription in *Bacillus thuringiensis* by γ-aminobutyric acid or succinic semialdehyde is mediated by the σ^{54}-dependent transcriptional activator GabR. *BMC Microbiol.* 14**,** 306. doi: 10.1186/s12866-014-0306-3.

Pennacchietti, E., D'Alonzo, C., Freddi, L., Occhialini, A., and De Biase, D. (2018). The glutaminase-dependent acid resistance system: qualitative and quantitative assays and analysis of its distribution in enteric bacteria. *Front. Microbiol.* 9**,** 2869. doi: 10.3389/fmicb.2018.02869.

Pfeifer-Sancar, K., Mentz, A., Rückert, C., and Kalinowski, J. (2013). Comprehensive analysis of the *Corynebacterium glutamicum* transcriptome using an improved RNAseq technique. *BMC Genomics* 14**,** 888. doi: 10.1186/1471-2164-14-888.

Reddy, M.C., Gokulan, K., Jacobs, W.R., Jr., Ioerger, T.R., and Sacchettini, J.C. (2008). Crystal structure of *Mycobacterium tuberculosis* LrpA, a leucine-responsive global regulator associated with starvation response. *Protein Sci.* 17(1)**,** 159-170. doi: 10.1110/ps.073192208.

Rehm, N., and Burkovski, A. (2011). Engineering of nitrogen metabolism and its regulation in *Corynebacterium glutamicum*: influence on amino acid pools and production. *Appl. Microbiol. Biotechnol.* 89(2)**,** 239-248. doi: 10.1007/s00253-010-2922-7.

Rehm, N., Georgi, T., Hiery, E., Degner, U., Schmiedl, A., Burkovski, A., et al. (2010). L-Glutamine as a nitrogen source for *Corynebacterium glutamicum*: derepression of the AmtR regulon and implications for nitrogen sensing. *Microbiology* 156**,** 3180-3193. doi: Doi 10.1099/Mic.0.040667-0.

Richhardt, J., Bringer, S., and Bott, M. (2012). Mutational analysis of the pentose phosphate and Entner-Doudoroff pathways in *Gluconobacter oxydans* reveals improved growth of a Δedd Δeda mutant on mannitol. *Appl. Environ. Microbiol.* 78(19)**,** 6975-6986. doi: 10.1128/AEM.01166-12.

Riedel, C., Rittmann, D., Dangel, P., Möckel, B., Petersen, S., Sahm, H., et al. (2001). Characterization of the phosphoenolpyruvate carboxykinase gene from *Corynebacterium glutamicum* and significance of the enzyme for growth and amino acid production. *J.Mol. Microbiol.Biotechnol.* 3(4)**,** 573-583.

Sainsbury, S., Lane, L.A., Ren, J., Gilbert, R.J., Saunders, N.J., Robinson, C.V., et al. (2009). The structure of CrgA from *Neisseria meningitidis* reveals a new octameric assembly state for LysR transcriptional regulators. *Nucleic Acids Res.* 37(14)**,** 4545-4558. doi: 10.1093/nar/gkp445.

Sambrook, J., Fritsch, E.F., and Maniatis, T. (1989). *Molecular Cloning. A Laboratory Manual.* Cold Spring Harbor, New York: Cold Spring Harbor Laboratory Press.

Schäfer, A., Tauch, A., Jäger, W., Kalinowski, J., Thierbach, G., and Pühler, A. (1994). Small mobilizable multipurpose cloning vectors derived from the *Escherichia coli* plasmids pK18 and pK19 - Selection of defined deletions in the chromosome of *Corynebacterium glutamicum*. *Gene* 145(1)**,** 69-73.

Schneider, B.L., and Reitzer, L. (2012). Pathway and enzyme redundancy in putrescine catabolism in *Escherichia coli. J. Bacteriol.* 194(15)**,** 4080-4088. doi: 10.1128/JB.05063-11.

Schneider, B.L., Ruback, S., Kiupakis, A.K., Kasbarian, H., Pybus, C., and Reitzer, L. (2002). The *Escherichia coli gabDTPC* operon: specific γ-aminobutyrate catabolism and nonspecific induction. *J. Bacteriol.* 184(24)**,** 6976-6986. doi: 10.1128/jb.184.24.6976-6986.2002.

994 Schultz, A.C., Nygaard, P., and Saxild, H.H. (2001). Functional analysis of 14 genes that constitute the
995   purine catabolic pathway in *Bacillus subtilis* and evidence for a novel regulon controlled by the
996   PucR transcription activator. *J. Bacteriol.* 183(11)**,** 3293-3302. doi: 10.1128/JB.183.11.3293-
997   3302.2001.

998 Scott, E.M., and Jakoby, W.B. (1958). Pyrrolidine metabolism - soluble γ-aminobutyric transaminase
999   and semialdehyde dehydrogenase. *Science* 128(3320)**,** 361-362. doi: DOI
1000   10.1126/science.128.3320.361-a.

1001 Shi, F., Jiang, J., Li, Y., Li, Y., and Xie, Y. (2013). Enhancement of γ-aminobutyric acid production in
1002   recombinant *Corynebacterium glutamicum* by co-expressing two glutamate decarboxylase
1003   genes from *Lactobacillus brevis*. *J. Ind. Microbiol. Biotechnol.* 40(11)**,** 1285-1296. doi:
1004   10.1007/s10295-013-1316-0.

1005 Shi, F., and Li, Y. (2011). Synthesis of γ-aminobutyric acid by expressing *Lactobacillus brevis*-derived
1006   glutamate decarboxylase in the *Corynebacterium glutamicum* strain ATCC 13032. *Biotechnol.*
1007   *Lett.* 33(12)**,** 2469-2474. doi: 10.1007/s10529-011-0723-4.

1008 Shi, F., Si, H., Ni, Y.L., Zhang, L., and Li, Y.F. (2017). Transaminase encoded by NCgl2515 gene of
1009   *Corynebacterium glutamicum* ATCC 13032 is involved in γ-aminobutyric acid decomposition.
1010   *Process Biochem.* 55**,** 55-60. doi: 10.1016/j.procbio.2017.01.016.

1011 Shiio, I., and Ozaki, H. (1970). Regulation of nicotinamide adenine dinucleotide phosphate-specific
1012   glutamate dehydrogenase from *Brevibacterium flavum*, a glutamate-producing bacterium. *J.*
1013   *Biochem.* 68(5)**,** 633-647.

1014 Siewe, R.M., Weil, B., Burkovski, A., Eggeling, L., Krämer, R., and Jahns, T. (1998). Urea uptake and
1015   urease activity in *Corynebacterium glutamicum*. *Arch. Microbiol.* 169(5)**,** 411-416.

1016 Song, N., Cui, Y., Li, Z., Chen, L., and Liu, S. (2016). New targets and cofactors for the transcription
1017   factor LrpA from *Mycobacterium tuberculosis*. *DNA Cell Biol.* 35(4)**,** 167-176. doi:
1018   10.1089/dna.2015.3040.

1019 Strandwitz, P., Kim, K.H., Terekhova, D., Liu, J.K., Sharma, A., Levering, J., et al. (2019). GABA-
1020   modulating bacteria of the human gut microbiota. *Nat Microbiol* 4(3)**,** 396.

1021 Strösser, J., Lüdke, A., Schaffer, S., Krämer, R., and Burkovski, A. (2004). Regulation of GlnK activity:
1022   modification, membrane sequestration and proteolysis as regulatory principles in the network
1023   of nitrogen control in *Corynebacterium glutamicum*. *Mol. Microbiol.* 54**,** 132-147.

1024 Studier, F.W., and Moffatt, B.A. (1986). Use of bacteriophage T7 RNA polymerase to direct selective
1025   high-level expression of cloned genes. *J. Mol. Biol.* 189**,** 113-130.

1026 Takahashi, C., Shirakawa, J., Tsuchidate, T., Okai, N., Hatada, K., Nakayama, H., et al. (2012). Robust
1027   production of γ-amino butyric acid using recombinant *Corynebacterium glutamicum* expressing
1028   glutamate decarboxylase from *Escherichia coli*. *Enzyme Microb. Technol.* 51(3)**,** 171-176. doi:
1029   10.1016/j.enzmictec.2012.05.010.

1030 Toyoda, K., Teramoto, H., Inui, M., and Yukawa, H. (2011). Genome-wide identification of *in vivo*
1031   binding sites of GlxR, a cyclic AMP receptor protein-type regulator in *Corynebacterium*
1032   *glutamicum*. *J. Bacteriol.* 193**,** 4123-4133. doi: 10.1128/JB.00384-11.

1033 van der Rest, M.E., Lange, C., and Molenaar, D. (1999). A heat shock following electroporation induces
1034   highly efficient transformation of *Corynebacterium glutamicum* with xenogeneic plasmid DNA.
1035   *Appl. Microbiol. Biotechnol.* 52(4)**,** 541-545.

1036 Vogt, M., Haas, S., Klaffl, S., Polen, T., Eggeling, L., van Ooyen, J., et al. (2014). Pushing product
1037   formation to its limit: Metabolic engineering of *Corynebacterium glutamicum* for L-leucine
1038   overproduction. *Metab. Eng.* 22**,** 40-52. doi: 10.1016/j.ymben.2013.12.001.

1039 Walter, B., Kuspert, M., Ansorge, D., Krämer, R., and Burkovski, A. (2008). Dissection of ammonium
1040   uptake systems in *Corynebacterium glutamicum*: Mechanism of action and energetics of AmtA
1041   and AmtB. *J. Bacteriol.* 190(7)**,** 2611-2614.

1042 Wendisch, V.F., De Graaf, A.A., Sahm, H., and Eikmanns, B.J. (2000). Quantitative determination of
1043   metabolic fluxes during coutilization of two carbon sources: comparative analyses with
1044   *Corynebacterium* glutamicum during growth on acetate and/or glucose. *J. Bacteriol.* 182(11)**,**
1045   3088-3096.

1046 Wennerhold, J., and Bott, M. (2006). The DtxR regulon of *Corynebacterium glutamicum*. *J. Bacteriol.*
1047   188**,** 2907-2918.

1048 Wennerhold, J., Krug, A., and Bott, M. (2005). The AraC-type regulator RipA represses aconitase and
1049   other iron proteins from *Corynebacterium* under iron limitation and is itself repressed by DtxR.
1050   *J. Biol. Chem.* 280(49)**,** 40500-40508.

1051 Wolf, N., Bussmann, M., Koch-Koerfges, A., Katcharava, N., Schulte, J., Polen, T., et al. (2020).
1052   Molecular basis of growth inhibition by acetate of an adenylate cyclase-deficient mutant of
1053   *Corynebacterium glutamicum. Front. Microbiol.* 11(87). doi: 10.3389/fmicb.2020.00087.

1054 Wu, R., Sanishvili, R., Belitsky, B.R., Juncosa, J.I., Le, H.V., Lehrer, H.J., et al. (2017). PLP and GABA
1055   trigger GabR-mediated transcription regulation in *Bacillus subtilis* via external aldimine
1056   formation. *Proc. Natl. Acad. Sci. USA* 114(15)**,** 3891-3896. doi: 10.1073/pnas.1703019114.

1057 Xu, N., Wei, L., and Liu, J. (2017). Biotechnological advances and perspectives of γ-aminobutyric acid
1058   production. *World J. Microbiol. Biotechnol.* 33(3)**,** 64. doi: 10.1007/s11274-017-2234-5.

1059 Zhao, Z., Ding, J.Y., Ma, W.H., Zhou, N.Y., and Liu, S.J. (2012). Identification and characterization of
1060   γ-aminobutyric acid uptake system $GabP_{Cg}$ (NCgl0464) in *Corynebacterium glutamicum. Appl.*
1061   *Environ. Microbiol.* 78**,** 2596-2601. doi: 10.1128/AEM.07406-11.

1062 Zhu, L. (2020). *γ-Aminobutyrate as carbon and nitrogen source for Corynebacterium glutamicum and*
1063   *regulation of the catabolic genes by GabR.* Doctoral thesis, University of Düsseldorf.

1064 Zhu, L., Peng, Q., Song, F., Jiang, Y., Sun, C., Zhang, J., et al. (2010). Structure and regulation of the
1065   *gab* gene cluster, involved in the γ-aminobutyric acid shunt, are controlled by a σ^{54} factor in
1066   *Bacillus thuringiensis. J. Bacteriol.* 192(1)**,** 346-355. doi: 10.1128/JB.01038-09.

1067

1068 **TABLE 1.** Bacterial strains and plasmids used in this study

Strain or plasmid	Relevant characteristics	Source or reference
E. coli		
DH5α	F⁻ Φ80*dlac*Δ(*lacZ*)M15 Δ(*lacZYA-argF*) U169 *endA1 recA1 hsdR17* (r$_K^-$, m$_K^+$) *deoR thi-1 phoA supE44* λ⁻ *gyrA96 relA1*; strain used for cloning procedures	(Hanahan, 1983)
BL21(DE3)	F- *ompT hsdS*$_B$ (r$_B$-, m$_B$-) *gal dcm* (DE3); host for protein production	(Studier and Moffatt, 1986)
C. glutamicum		
ATCC 13032 (Cg WT)	Biotin-auxotrophic wild type	(Kinoshita et al., 1957)
Δ*gabR*	WT derivative with an in-frame deletion of *gabR* (cg0565)	This work
Δ*gdh* (LNΔGDH)	ATCC 13032 with deletion of *gdh* (cg2280)	(Müller et al., 2006)
Δ*glnA* (LNΔGS)	ATCC13032 with deletion of *glnA* (cg2429)	(Müller et al., 2006)
Δ*gltBD* (LNΔ*gltBD*)	ATCC13032 with deletion of *gltB* (cg0229) and *gltD* (cg0230)	(Rehm et al., 2010)
Δ*glnA*Δ*glnA2*Δ*gdh* (DA-2)	ATCC13032 with deletion of *gdh* (cg2280), *glnA* (cg2429) and *glnA*2 (cg2477)	(Walter et al., 2008)
Plasmids		
pK19*mobsacB*	Kan^R; plasmid for allelic exchange in *C. glutamicum*; (pK18 *oriV$_{E.c.}$*, *sacB*, *lacZ*α)	(Schäfer et al., 1994)
pK19*mobsacB*-Δ*gabR*	Kan^R.; pK19mobsacB derivative containing a PCR product covering the up- and downstream regions of *gabR* (cg0565)	This work
pAN6	Kan^R; *C. glutamicum*/*E. coli* shuttle vector for regulated gene expression using the P$_{tac}$ promoter, derivative of pEKEx2.	(Frunzke et al., 2008)
pAN6-*gabR*	Kan^R; pAN6 derivative for expression of *gabR* (cg0565) under control of P$_{tac}$	This work
pAN6-*gabTDP*	Kan^R; pAN6 derivative for expression of *gabTDP* cluster	This work
pET-TEV	Kan^R; pET28b derivative for overexpression of genes in E. coli, adding an N-terminal decahistdine tag and a TEV protease cleavage site to the target protein (pBR322 oriVE.c., PT7, lacI)	(Bussmann et al., 2010)
pET-TEV-*gabR*	Kan^R; pET-TEV derivative for overproduction of GabR (cg0565)	This work
pJC1-P$_{tac}$-*eyfp*	Kan^R; pJC1 derivative containing the *eyfp* gene under the control of P$_{tac}$	(Kortmann et al., 2015)
pJC1-venus-term	Kan^R; *E. coli-C. glutamicum* shuttle vector, pJC1 derivative carrying the venus coding sequence and additional terminators	(Baumgart et al., 2013)

38

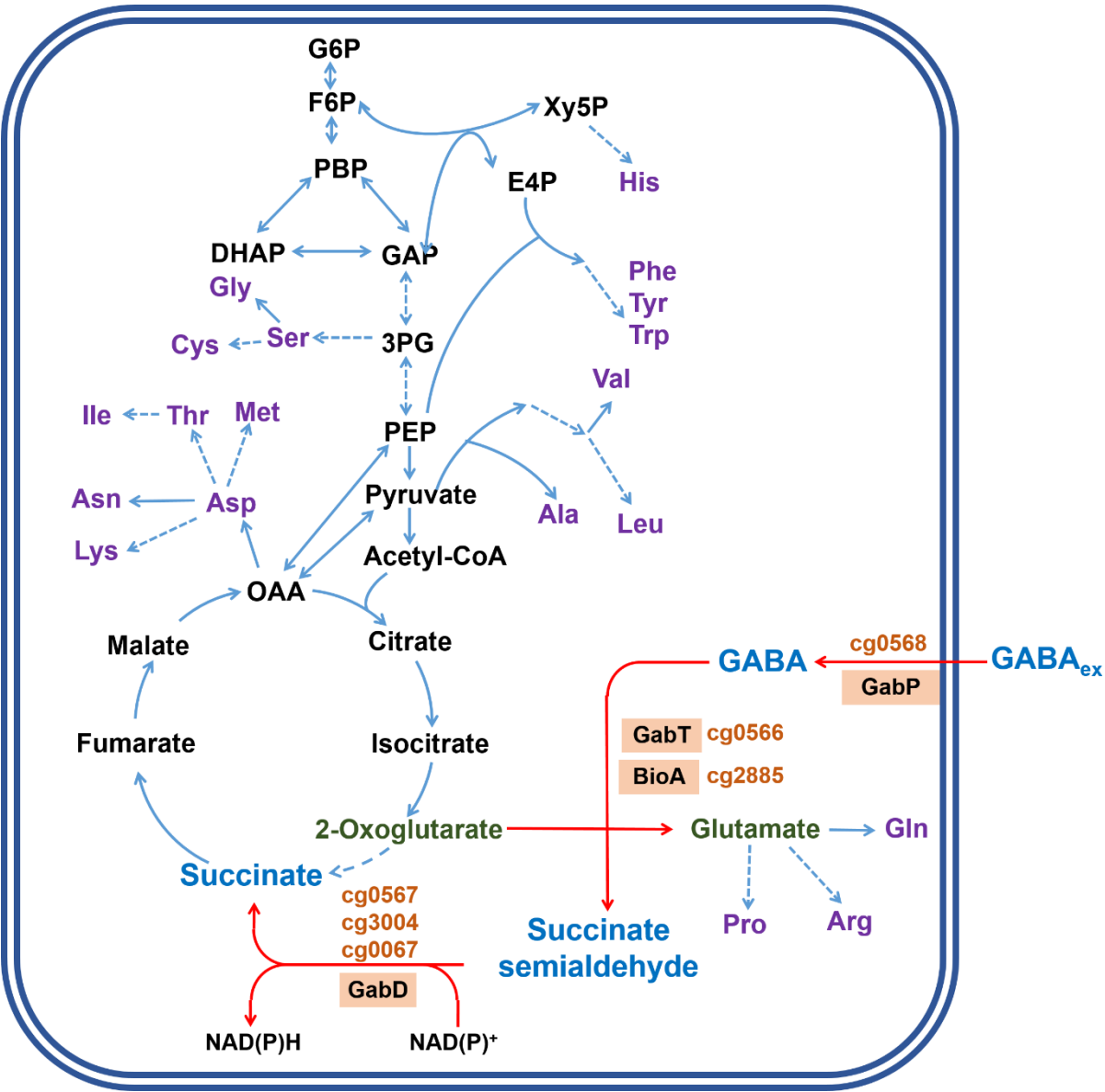| pJC1-P$_{gabT}$-eYFP | Kan^R; pJC1-venus-term derivative carrying the promoter of *gabT* (cg0566) fused to *eyfp* | This work |
| pJM0462 | Cm^R; pASK-IBA-3C derivative with the coding sequence of *gabT* (cg0566, NCgl0462) | (Marienhagen et al., 2005) |

1069

FIGURE LEGENDS

FIGURE 1. Model of GABA metabolism in *C. glutamicum* and integration into central metabolism. The metabolites and reactions specifically involved in GABA metabolism are indicated by blue letters and red arrows, respectively. The proteins involved in GABA transport and degradation and the corresponding locus tags are indicated in orange. GabP is a sodium ion-coupled secondary transporter for GABA uptake (Zhao et al., 2012). GabT functions as γ-aminobutyrate aminotransferase (Shi et al., 2017). BioA (cg2885) was reported to also possess some GABA aminotransferase activity (Shi et al., 2017). GabD (cg0567) as well as two further proteins encoded by cg0067 and cg3004 are annotated as succinate semialdehyde

1080   dehydrogenase (Kalinowski et al., 2003). $GABA_{ex}$ represents extracellular GABA. Metabolites

1081   involved in central metabolism are shown in black letters, amino acids in purple letters. Solid

1082   blue arrows indicate conversions catalyzed by a single enzyme, dashed lines represents

1083   conversions composed of several enzymatic steps. Abbreviations: DHAP, dihydroxyacetone

1084   phosphate; E4P, erythrose 4-phosphate; F6P, fructose 6-phosphate; FBP, fructose 1,6-

1085   bisphosphate; GAP, glyceraldehyde 3-phosphate; G6P, glucose 6-phosphate; OAA,

1086   oxaloacetate; PEP, phosphoenolpyruvate; 3PG, 3-phosphoglycerate; Xy5P, xylulose 5-

1087   phosphate.

1088
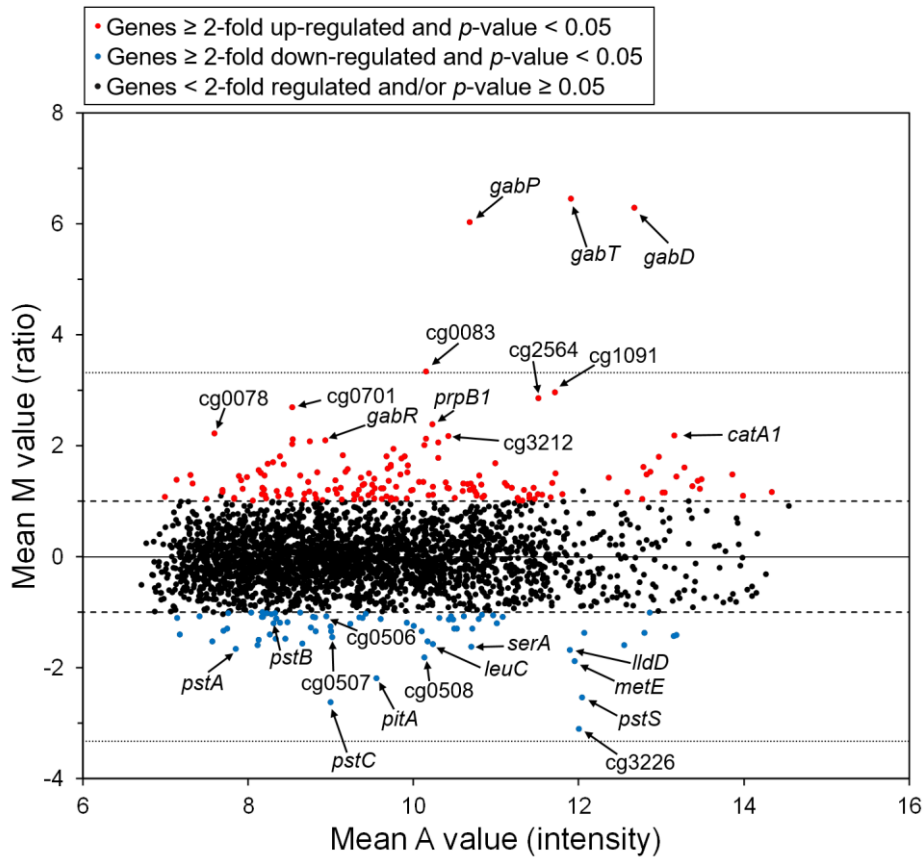
FIGURE 2. M/A plot showing differential gene expression in *C. glutamicum* WT cells grown with GABA and urea compared to WT cells grown with glucose and urea. The data shown are based on four two-channel DNA microarray hybridizations starting with cDNA from four independent biological replicates. The dashed lines indicate a 2-fold altered mRNA ratio, the dotted lines a 10-fold altered mRNA ratio.
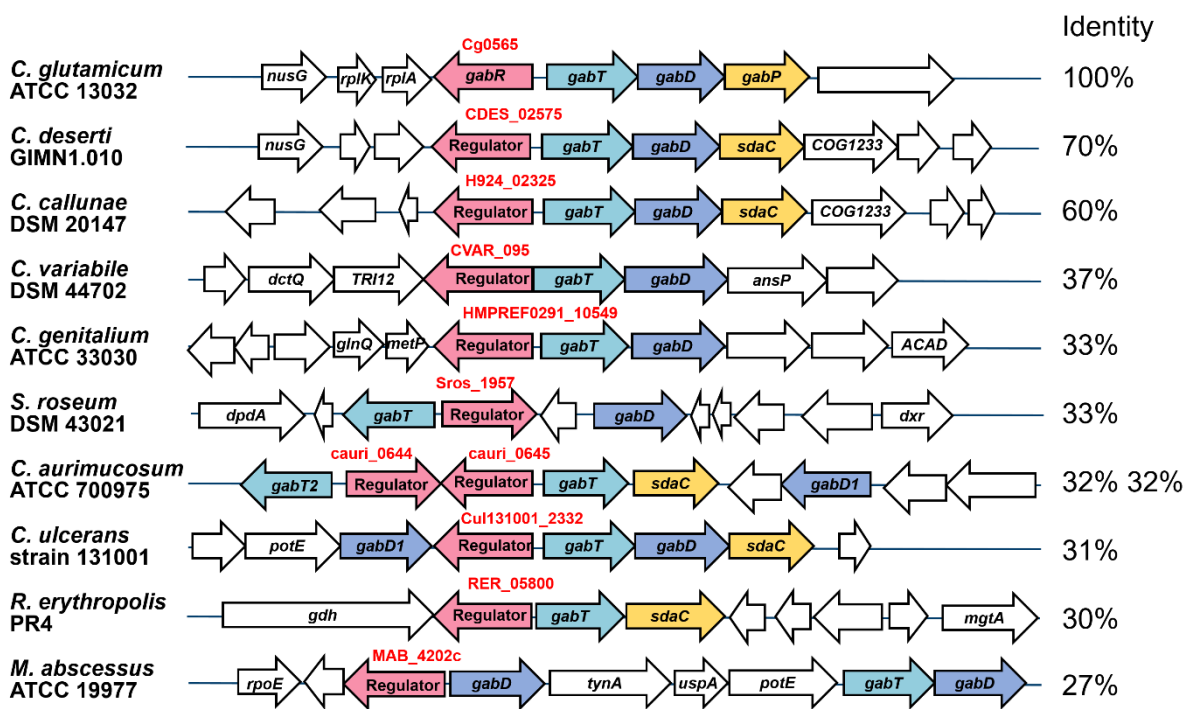
FIGURE 3. Genomic organization of the *gabR-gabTDP* gene cluster in different *Corynebacterium* species. Conserved genes are marked with different colors: *gabT* (γ-aminobutyrate aminotransferase, light blue), *gabD* (succinate semialdehyde dehydrogenase, blue), *gabP* or *sdaC* (GABA-specific importer, yellow), *gabR* (transcriptional regulator, red). Non-conserved genes located next to the *gabR-gabTDP* cluster are shown colorless. The amino acid sequence identity of GabR homologs with GabR of *C. glutamicum*, which was calculated by MultiGeneBlast (Medema et al., 2013), is given on the right. For *C. aurimucosum,* identity for both GabR homologs is given. The sequences were derived from the following genomes: *Corynebacterium deserti* GIMN1.010 (NZ_CP009220), *Corynebacterium callunae* DSM 20147 (NC_020506), *Corynebacterium variabile* DSM 44702 (NC_015859), *Corynebacterium genitalium* ATCC 33030 (NZ_CM000961), *Streptosporangium roseum* DSM 43021 (NC_013595), *Corynebacterium aurimucosum* ATCC 700975 (NC_012590), *Corynebacterium ulcerans* strain 131001 (NZ_CP010818), *Rhodococcus erythropolis* PR4 (NC_012490) and *Mycobacterium abscessus* ATCC 19977 (CU458896). The figure was generated using MultiGeneBlast (Medema et al., 2013).

43
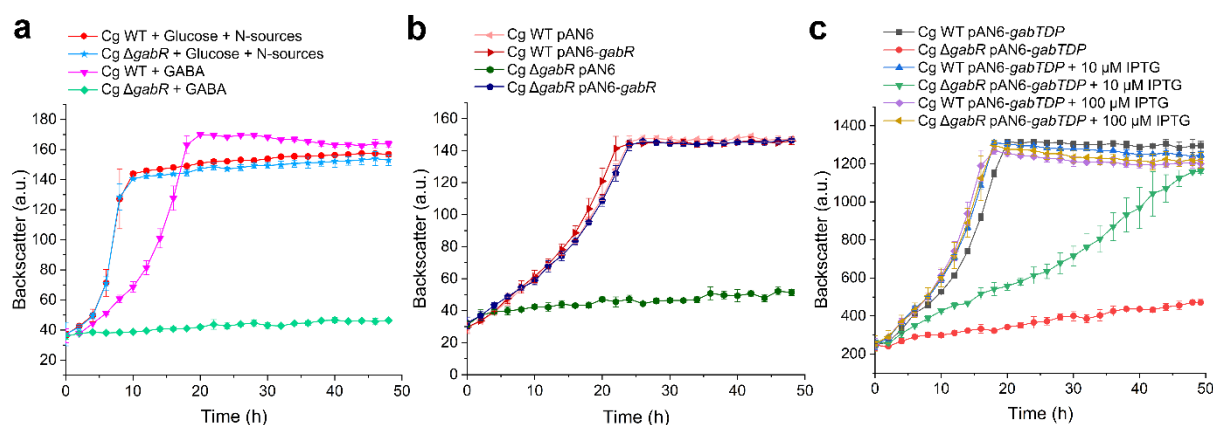
FIGURE 4. Growth studies with *C. gutamicum* WT and the ΔgabR mutant with or without the plasmids pAN6, pAN6-*gabR*, or pAN6-*gabTDP*. All strains were precultivated in BHIS medium and washed with phosphate buffer before inoculation of the main culture. Growth experiments were performed in a BioLector microcultivation system using 48-well Flower plates containing 750 µl CGXII minimal medium with 62.5 mM GABA as sole carbon and nitrogen source or with 41.7 mM glucose as carbon source and 151 mM $(NH_4)_2SO_4$ and 83 mM urea as nitrogen sources. (a) Growth of the *C. glutamicum* ΔgabR mutant compared to the WT with glucose or GABA as carbon sources. (b) Influence of plasmids pAN6 and pAN6-*gabR* on growth of *C. glutamicum* WT and the ΔgabR mutant with GABA as sole carbon and nitrogen source. (c) Influence of plasmids pAN6 and pAN6-*gabTDP* on growth of *C. glutamicum* WT and the ΔgabR mutant with GABA as sole carbon and nitrogen source. Where indicated, 10 µM or 100 µM IPTG was added to the medium for induction of the P_{tac} promoter controlling expression of *gabTDP*. Since the promoter of pAN6 is known to be slightly leaky, basal transcription of the target genes is independent of IPTG addition. Mean values and standard deviations of three biological replicates are shown.
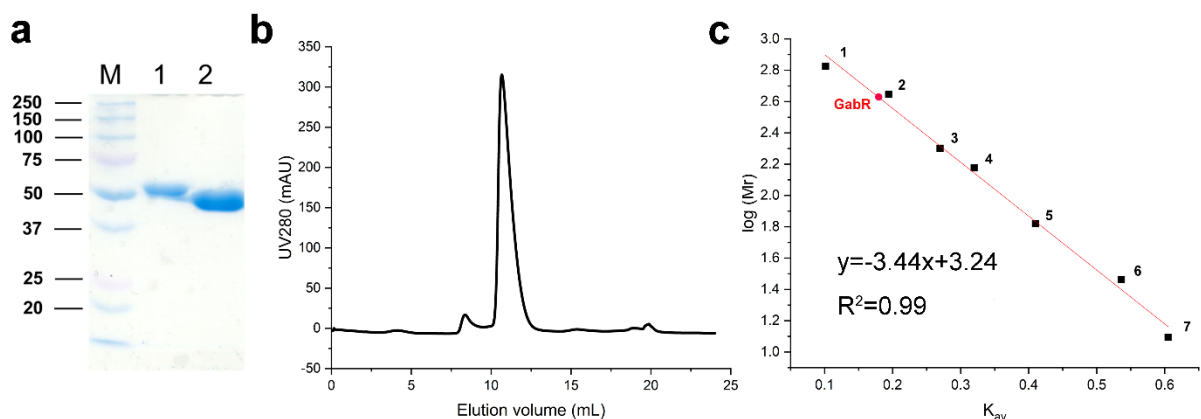
1128

FIGURE 5. Purification of GabR and determination of its native molecular mass. (a) Coomassie-stained SDS-polyacrylamide gel showing marker proteins (M, molecular mass in kDa) and GabR after Ni-NTA affinity chromatography (lane 1) and after His-tag removal with TEV protease (lane 2). (b) Size exclusion chromatography of tag-free GabR using a Superdex 200 Increase 10-300GL column (GE Healthcare). Protein was detected by absorbance at 280 nm. (c) Calibration curve for the Superdex column obtained with standard proteins: 1, thyroglobulin (669 kDa); 2, apoferritin (443 kDa); 3, amylase (200 kDa); 4, alcohol dehydrogenase (150 kDa); 5, bovine serum albumin (66 kDa); 6, carbonic anhydrase (29 kDa); 7, cytochrome c (12.4 kDa). The K_{av} value determined for GabR is marked with a red dot.

1138

45
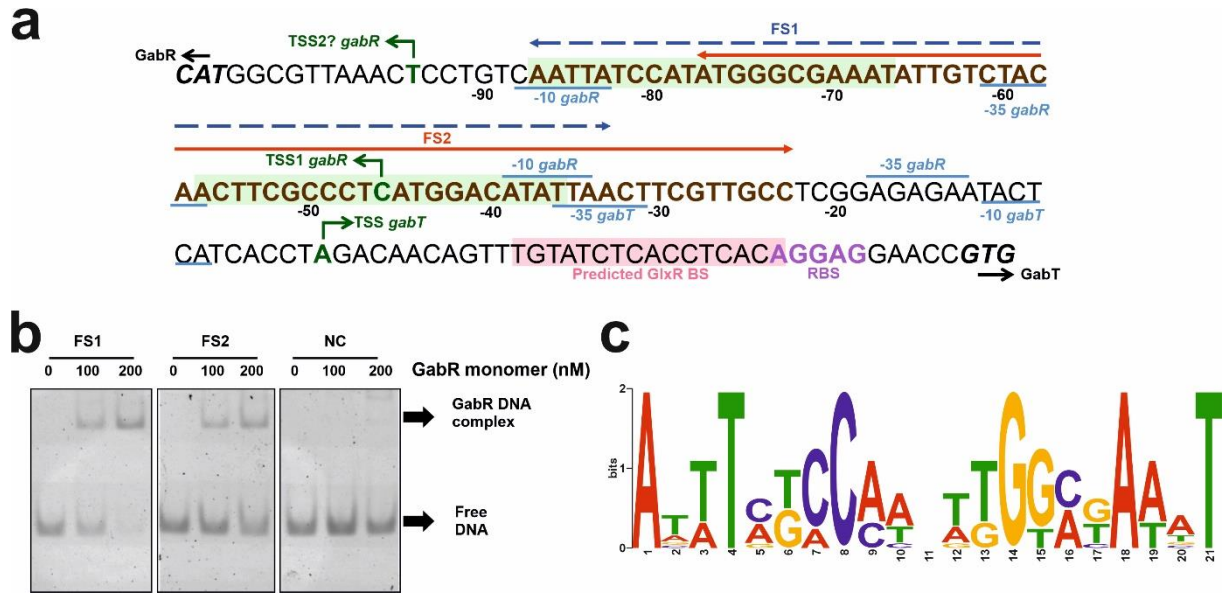
FIGURE 6. Determination of the binding site(s) of GabR in the *gabTDP* promoter region. (a) Sequence of the *gabR-gabT* intergenic region. The ATG start codon of *gabR* (cg0565) and the GTG start codon of *gabT* (cg0566) are shown in bold and italic. The transcriptional start sites of *gabR* and *gabT* are indicated with green arrows. The corresponding -10 and -35 regions are labeled in blue. The ribosome binding site of *gabTDP* is labeled in purple, and the predicted GlxR binding site is marked with light red background. The binding region for GabR determined in this work by EMSAs is marked in bold brown letters (compare Fig. S3). Fragments FS1 (-87 to -33) and FS2 (-77 to -23) are marked in the figure by a blue or red arrow, respectively. Potential binding sites for GabR are marked with light green background. (b) EMSAs with purified GabR and DNA fragments FS1 and FS2. The fragments were incubated with the indicated GabR concentrations (given in nM of monomers). A 55 bp fragment downstream of the predicted binding sites was used as negative control (NC). (c) Proposed GabR consensus binding site identified with MEME software using the *gabR-gabT* intergenic regions of *C. glutamicum* WT, *Corynebacterium deserti* and *Corynebacterium callunae* as input sequences.
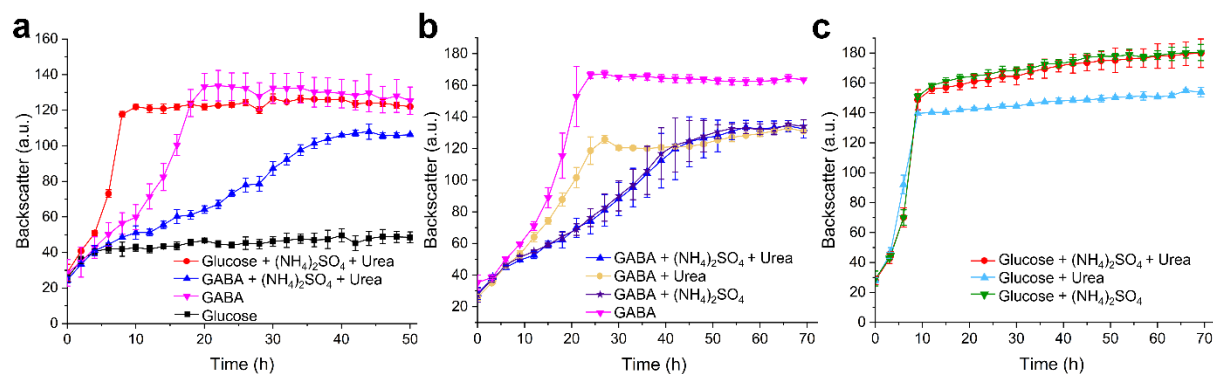
FIGURE 7. Growth of *C. glutamicum* WT with different carbon and nitrogen sources. Cells were precultured in BHIS medium for 12 hours and subsequently washed with phosphate buffer before inoculation of the main cultures to a starting OD_{600} of 0.5. The main cultivation was performed in a BioLector microcultivation system with 48-well Flower plates each containing 750 µL CGXII minimal medium supplemented with 41.7 mM glucose or 62.5 mM GABA. 151 mM $(NH_4)_2SO_4$ or 83 mM urea were included as indicated. Mean values and standard deviations of three biological replicates are shown.

47
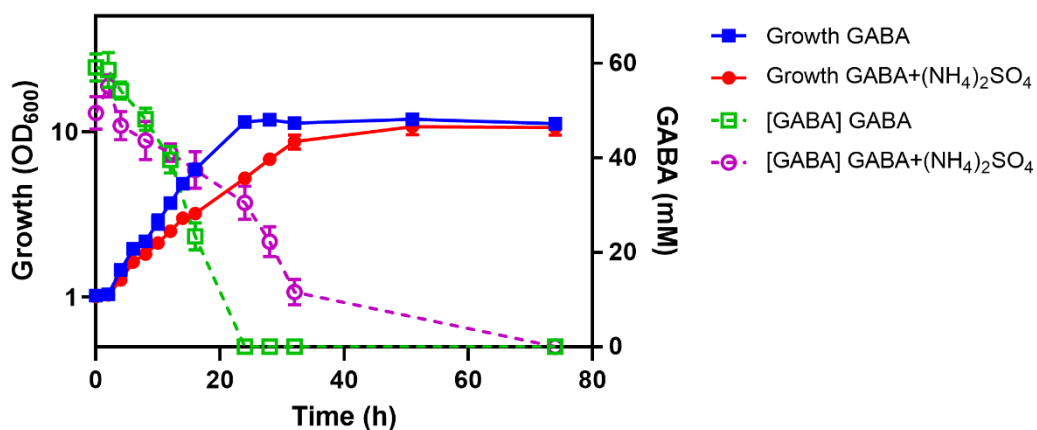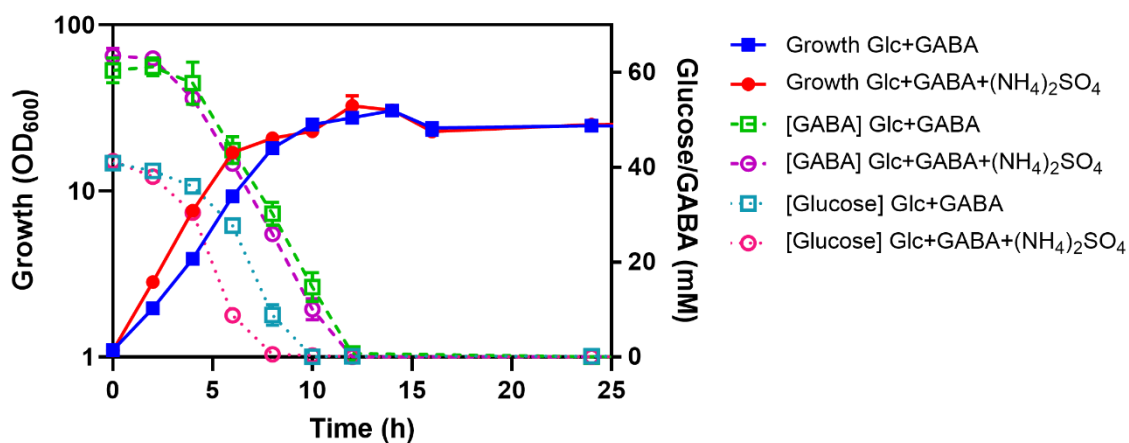
FIGURE 8. Influence of $(NH_4)_2SO_4$ on GABA consumption in the absence (A) and presence (B) of glucose (Glc). *C. glutamicum* WT was cultured in shake flasks containing CGXII medium with the indicated carbon and nitrogen sources (62.5 mM GABA, 41.7 mM glucose, 151 mM $(NH_4)_2SO_4$). Glucose and GABA concentrations were determined by HPLC. Mean values and standard deviations of three biological replicates are shown.
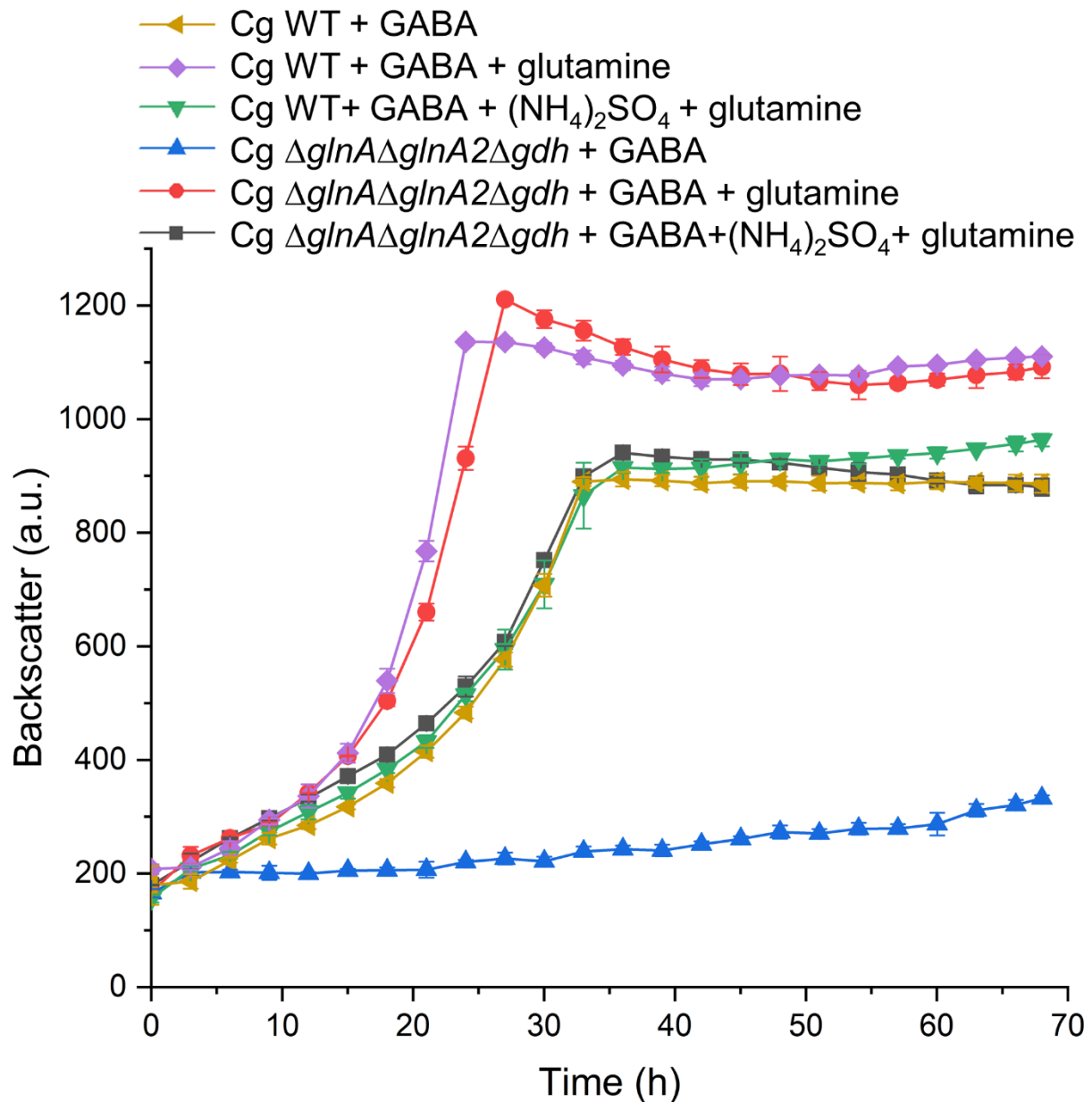
48

FIGURE 9. Influence of L-glutamine supplementation on growth of *C. glutamicum* WT and the Δ*glnA*Δ*glnA2*Δ*gdh* mutant in CGXII medium with GABA. Cells were precultured in BHIS medium for 12 hours and subsequently washed with phosphate buffer before inoculation of the main cultures to a starting OD_{600} of 0.5. The main cultivation was performed in a BioLector microcultivation system with 48-well Flower plates each containing 750 µL CGXII minimal medium supplemented with 62.5 mM GABA. 20 mM L-glutamine and 151 mM $(NH_4)_2SO_4$ were included as indicated. For the WT mean values of three biological replicates are shown, for the mutant mean values of two biological replicates.
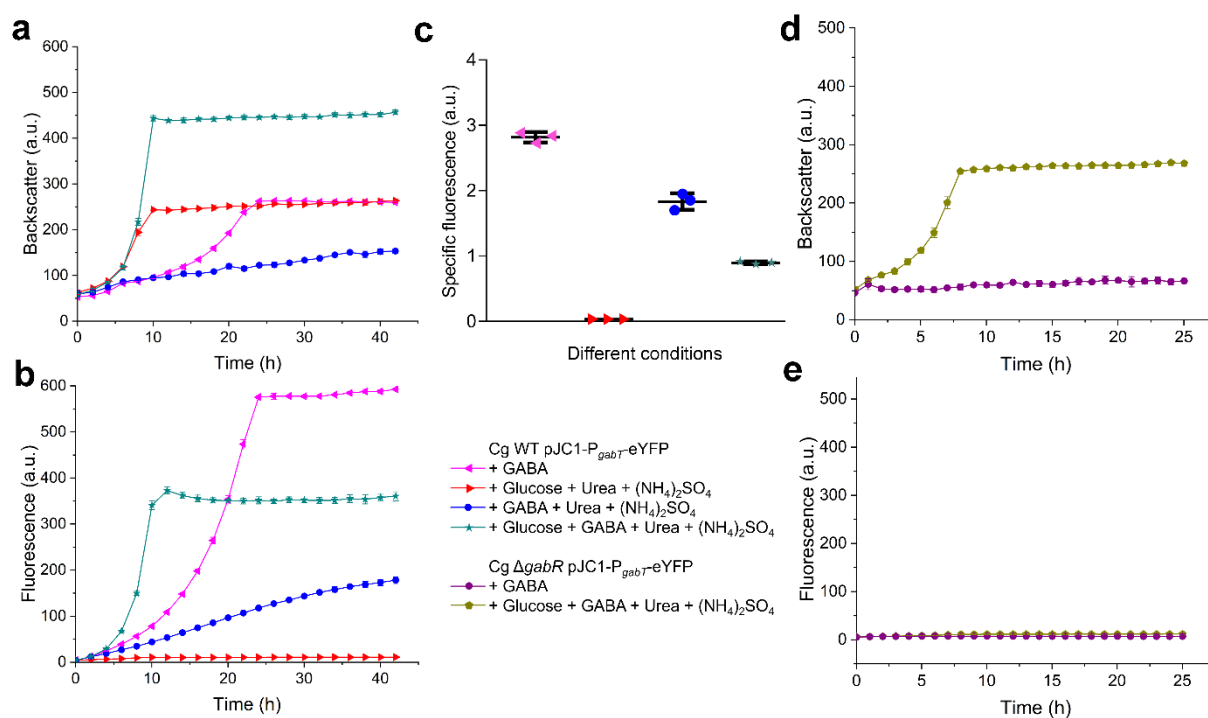
1178

FIGURE 10. Relevance of GabR for *gabTDP* transcription. *C. glutamicum* WT or the Δ*gabR*

mutant transformed with the reporter plasmid pJC1-P$_{gabT}$-eYFP were precultivated in BHIS

medium and washed with phosphate buffer before inoculation of the main cultures. The

cultivations were performed in a BioLector microcultivation system at 30 °C and 1200 rpm

using 750 µl CGXII minimal medium supplemented with GABA (62.5 mM), glucose (41.7

mM), $(NH_4)_2SO_4$ (151 mM), and urea (83 mM) as indicated. (a, b) Growth and eYFP

fluorescence representing the activity of the *gabTDP* promoter of *C. glutamicum* WT with

pJC1-P$_{gabT}$-eYFP. (c) Specific fluorescence (ratio fluorescence/backscatter) of the cultures

shown in (a) and (b) after 40 h. (d, e) Growth and fluorescence *C. glutamicum* Δ*gabR* harboring

pJC1-P$_{gabT}$-eYFP. Mean values and standard deviations of three biological replicates are shown.
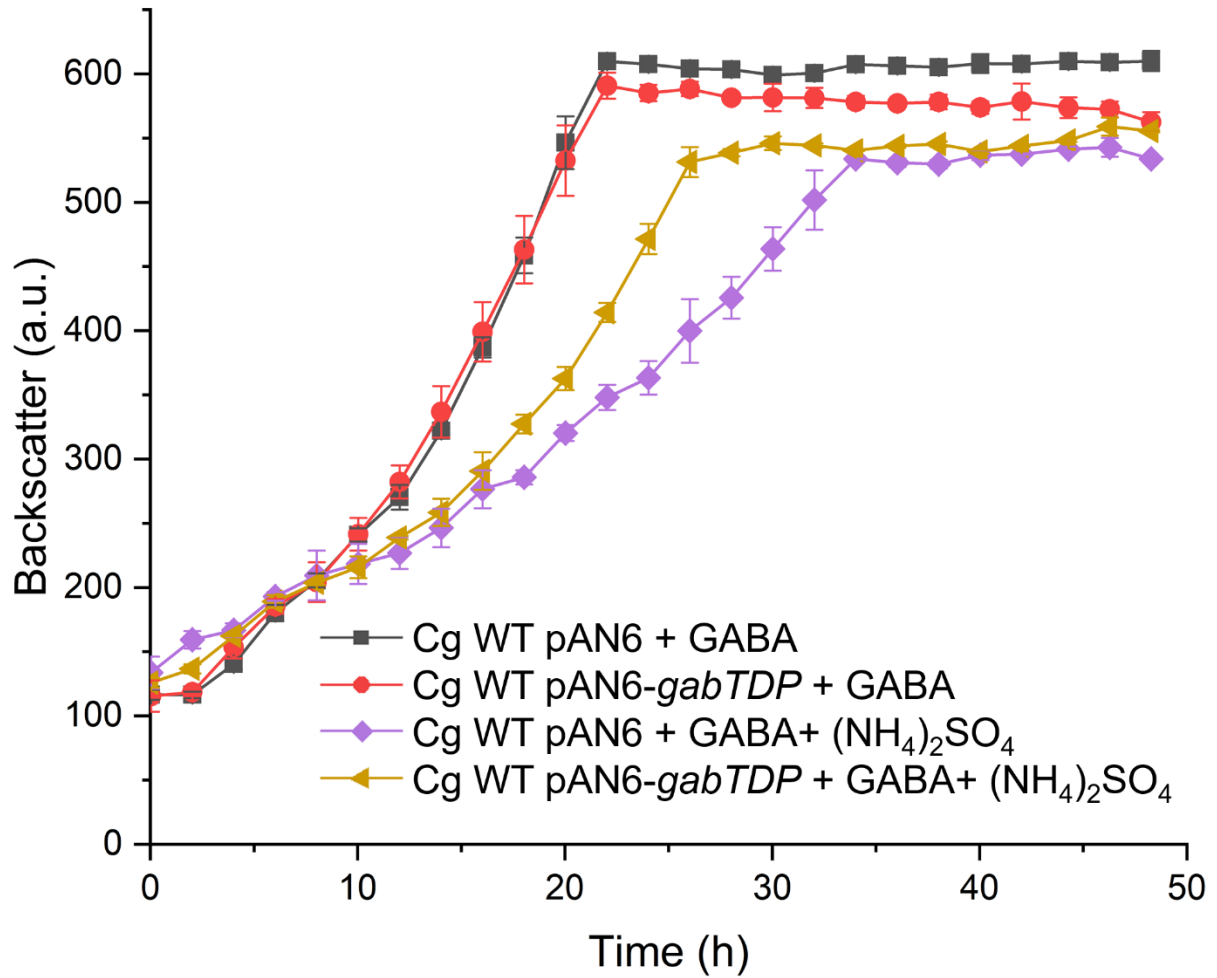
FIGURE 11. Growth of *C. glutamicum* WT harboring pAN6-*gabTDP* or pAN6 with different substrates in the presence of 10 μM IPTG. Growth experiments were performed in a BioLector microcultivation system with 48-well Flower plates containing 750 μL CGXII minimal medium supplemented with GABA (62.5 mM) and $(NH_4)_2SO_4$ (151 mM) as indicated. BHIS medium was used for precultures and the cells were washed with phosphate buffer before inoculation of the main culture. Mean values and standard deviations of three biological replicates are shown.